NTNU – Trondheim
Norwegian University of
Science and Technology

Intracellular Localization of Polymeric Nanoparticles and the Effect of Encapsulated Drug *in vitro*

Kjetil Viste Levik

Master of Science in Physics and Mathematics
Submission date: June 2015
Supervisor: Catharina de Lange Davies, IFY

Norwegian University of Science and Technology
Department of Physics

Preface

This thesis marks the end of my Master of Science in Applied Physics and Mathematics at Norwegian University of Science and Technology. The last few years I have specialised in biophysics and medical technology and it is assumed that the reader of this thesis have some basic knowledge in these fields of science. The thesis was carried out at the Department of Physics at NTNU and is part of a collaboration between NTNU, St. Olavs hospital and SINTEF. The collaboration is led by Professor Catharina de Lange Davies and is called "Multifunctional nanoparticles in diagnosis and therapy of cancer".

First of all I would like to thank my supervisor, Professor Catharina de Lange Davies for letting me write both my project thesis and master thesis on this topic. It is a field in biomedical research that I find very interesting. During the past year I have faced many challenges during the experimental work and in the process of writing and Catharina has always been willing to share her knowledge and guide me through the processes. For that I am very grateful. The experimental work in this thesis was mostly a continuation of work done by Einar Sulheim. I thank you for the guidance and thoughts you have provided this past year.

I would like to thank all of the participants on the nanoparticle group at biophysics at NTNU. The weekly meetings was very helpful and the discussions provided me with tools and knowledge in addition to make me even more interested in this field.

A special thanks to Kristin Grenstad Sæterbø and Astrid Bjørkøy for excellent training and assistance in the cell lab, the flow cytometer and the microscope.

To my friends and family; thanks for supporting me and believing in what I do.

Trondheim, June 2015
Kjetil Viste Levik

Abstract

Chemotherapy could be greatly improved if drug carriers could deliver the chemotherapeutic agents specifically to the cancer cells. SINTEF Materials and Chemistry have developed a novel, multimodal polymeric nanoparticle platform which is promising for drug delivery and other medical applications. In this thesis, nanoparticles made of biodegradable poly(butyl cyanoacrylate) were used to investigate intracellular localization of the nanoparticles. In addition, the effect of drug encapsulated in the nanoparticles was evaluated. PC3 cells and HeLa cells were used.

Confocal laser scanning microscopy was used to study colocalization between the nanoparticles and lysosomes. Lysosomes were stained with CellLight® Lysosomes-GFP, while the nanoparticles were loaded with the fluorescent dye NR668. Very few nanoparticles were taken up by PC3 cells, but most of them was found to colocalize with lysosomes. The results from these experiments strengthens the hypothesize of endocytotic uptake of the nanoparticles.

AlamarBlue® cell viability assay was used to study the impact of encapsulated drug on cell proliferation, while flow cytometry was used to assess the impact of encapsulated drug on the cell cycle distribution. Drug encapsulated in nanoparticles was found to work very similar to free drug. This indicates that the nanoparticles or the released drug are able to escape the lysosomes. In addition it proves that the encapsulation process does not alter this drug in such a way that it becomes ineffective.

Sammendrag

Kjemoterapi kan forbedres betydelig hvis nanopartikler kan brukes til å levere cellegift direkte til kreftceller. SINTEF Materialer og Kjemi har utviklet en ny type, multimodale nanopartikler, som er lovende for dette og andre medisinske applikasjoner. I denne oppgave er nanopartikler laget av biodegraderbar poly(butyl cyanoakrylate) brukt til studere den intracellulære lokalisasjonen av slike nanopartikler. I tillegg er effekten av cellegift innkapslet i nanopartikler forsket på. PC3 celler og HeLa celler ble brukt i forsøkene.

Konfokalmikroskopi ble brukt til å lete etter kolokalisasjon mellom nanopartiklene og lysosomer. Lysosomene ble farget med CellLight® Lysosomes-GFP og nanopartiklene inneholdt fargestoffet NR668. Veldig lite opptak av nanopartikler ble observert i cellene, men de få som ble tatt opp var kolokalisert med lysosomer i nesten alle tilfellene. Resultatet fra disse eksperimentene styrker teorien, som er at disse pariklene blir tatt opp ved endocytose.

AlamarBlue® ble brukt til å studere innvirkningen av cellegift innkapslet i nanopartikler på celleoverlevelse. Flow cytometri ble brukt til å etterforske innvirkningen av innkapslet cellegift på cellesyklusen. Det ble funnet at cellegift innkapslet i nanopartikler virket veldig likt som fritt cellegift. Det beviser at innkapslingprosessen ikke ødelegger denne cellegiftens egenskaper.

Contents

List of abbreviations

AB ..... AlamarBlue®

BCA ..... Butyl cyanoacrylate

CA ..... Chemotherapeutic agent

CLL ..... CellLight® Lysosomes-GFP

CLSM ..... Confocal laser scanning microscopy

CME ..... Clathrin-mediated endocytosis

DMEM ..... Dulbecco's modified eagles medium

EPR ..... Enhanced permeability and retention

FCM ..... Flow cytometry

FF ..... Forward scatter

FLIM ..... Fluorescence lifetime imaging

IFP ..... Interstitial fluid pressure

MPS ..... Mononuclear phagocytic system

MRI ..... Magnetic resonance imaging

MW ..... Molecular weight

NP ..... Nanoparticle

PACA ..... Poly(alkyl cyanoacrylate)

PBCA ..... Poly(butyl cyanoacrylate)

PBS ..... Phosphate buffered saline

PEG ..... Poly(ethylene glycol)

PIHCA ..... Poly(isohexyl cyanoacrylate)

POCA ..... Poly(oktyl cyanoacrylate)

SS ..... Side scatter

STED ..... Stimulated emission depletion

Chapter 1

Introduction

Cancer is one of the leading causes of death worldwide, accounting for 8.2 million deaths in 2012. Despite having more knowledge about health and lifestyle choices that can reduce the risk of cancer, WHO expects about a 70 % increase in new cases over the next two decades [102]. Since its discovery there have been remarkable advances in modern medical sciences, but cancer remains a disease that is difficult to treat. Today's treatment is also known to have severe unwanted side effects. Cancer is a collective term used for cells having an unusual rapid growth, that can invade nearby tissue or form so called metastases.

Current treatment strategies involves chemotherapy, radiation, surgery, immunotherapy or a combination of these. While surgery is effective against solid tumors that have not spread to other tissues or organs, it is not always possible to carry out and there will always be a certain risk of complications. Both chemotherapy and radiation therapy lack specificity towards the cancer tissue and damage to healthy cells is inevitable. In all instances there is continuous improvement. The introduction of robot-assisted surgery have improved the precision in surgery and decreased the invasiveness. Proton therapy, which has become increasingly popular the last decade is known to give a more precisely localized dose compared to traditional radiation therapy. Although immunotherapy is the newest arrival in the fight against cancer, it already show great potential.

A goal in chemotherapy has been to develop personalized and tailored drugs. The idea is more than a hundred years old and Paul Ehrlich, by many known as the founder of chemotherapy, postulated the creation of what he called "magic bullets"

in the early 20th century [88]. Today the term "magic bullet" has been replaced by nanoparticle, but the idea of a compound being able to selectively target a disease-causing organism is still the same.

SINTEF Materials and Chemistry have developed such a novel drug delivery system based on biodegradable polymeric nanoparticles (PNPs). They are synthesized through a one-step miniemulsion polymerization process where surface functionalities, drugs, contrast agents and other functionalities are fairly easy to incorporate [62]. Scientists at the Department of Physics at NTNU have been studying these PNPs for some years know and in collaboration with SINTEF the particles are continuously being optimized.

So far much effort have been put into investigating the degradation and stability, the uptake and the cytoxicity of the particles both in vitro and in vivo [8] [84] [101] [89]. These particles have either been empty or loaded with a fluorescent probe to be able to track the particles. While there is still more knowledge to gather from studying such particles, the team felt confident to start working on particles loaded with real drug.

1.0.1 Project motivation

This master thesis had two purposes:

- Continue to study the intracellular fate of PNPs by staining organelles in the endocytotic machinery and look for colocalization with the particles. If colocalization was found, the degradation should be assessed.
- Investigate the cytoxicity of the chemotherapeutic agent, cabazitaxel, encapsulated in PNPs by looking at cell proliferation.

Chapter 2

Theory

2.1 Drug delivery

One of the most common cancer treatments is chemotherapy. This treatment involves the use of drugs to defeat a tumor or stop its growth. Traditional chemotherapeutic agents are cytotoxic, which means that they cause cell death to the cells they infiltrate. The biggest obstacle in using this treatment is that the agents infiltrate the healthy cells as well as the cancer cells. The fact that healthy cells are dying have a lot of unwanted side-effects.

One approach to optimize this treatment is the use of some carrier to deliver the drugs more efficiently to the cancer cells. The idea is to encapsulate the drug in some kind of capsule or particle. This capsule or particle must meet certain criteria to work as a drug delivery carrier: It needs to be biodegradable so it does not accumulate in the body. It needs to be biocompatible, which means no negative reactions when placed in the body. It have to be stable enough to reach the desired target before it is degraded. And it should be selective so it targets only the desired cells, or at least is seen in much higher concentrations in the desired cells compared to other cells.

2.1.1 Opsonization - first barrier for drug delivery

Most drug delivery carriers are foreign objects to our body and are attacked by the mononuclear phagocytic system (MPS) once they are administered into the bloodstream. The first step of the MPS is the binding of opsonin proteins to the

carrier surface. After the opsonization, a phagocyte attach to the carrier before it ingests it [69]. Since the initial opsonization is critical for the phagocyte recognition, much research have been conducted on avoiding or stop this step of the clearance process. This have resulted in stealth carriers and are described more in section 2.2.4.

2.1.2 Tumor tissue

As previously stated, one of the main difficulties with chemotherapy is for drug to distinguish between healthy cells and cancer cells. However, tumor tissue has some characteristics that easily separates it from normal tissue. Most of the characteristics originate from the fact that cancer cells have such a rapid growth. Rapid growth requires high throughput of oxygen and nutrients. Therefore cancer cells secrete pro-angiogenic factors to surrounding tissue, resulting in growth of new blood vessels that connect the tumor to the body's vascular system[63]. Because of the rapid growth, blood vessels found in tumor tissue are abnormal. They often have an irregular diameter and an abnormal branching pattern [54]. As normal vessels, they consist of endothelial cells and pericytes, but the endothelial cells do not form a normal monolayer. The gap between endothelial cells in healthy vessels are typically 5-10nm, while for vessels in cancerous tissue the gap can be as much as 2 μm [33]. This leads to fluid being able to leak out of the vessels.

A lot of research has been conducted on the lymphatic system in tumors to figure out how cancer spread to other locations. It has been found that intratumoral lymphatic vessels are very rare [70]. The cancer cells secrete pro-lymphangiogenic factors, but high mechanical forces generated by growing cancer cells makes the lymphatic vessels collapse.

Elevated interstitial fluid pressure (IFP) is a consequence of the architectural abnormalities described and are common in almost all solid tumors [31]. It forms a barrier for the transport of therapeutic agents from the blood vessels to the tumor which results in inefficient treatment. Increased IFP is also linked to lymph node metastasis [79]. Many types of treatments have shown to decrease this pressure by fixing the vascular system or altering the extracellular matrix in the tumors [31]. Increased IFP is also believed to be one of the main reasons for nutrient deprivation and hypoxia, which is common in tumors [79].

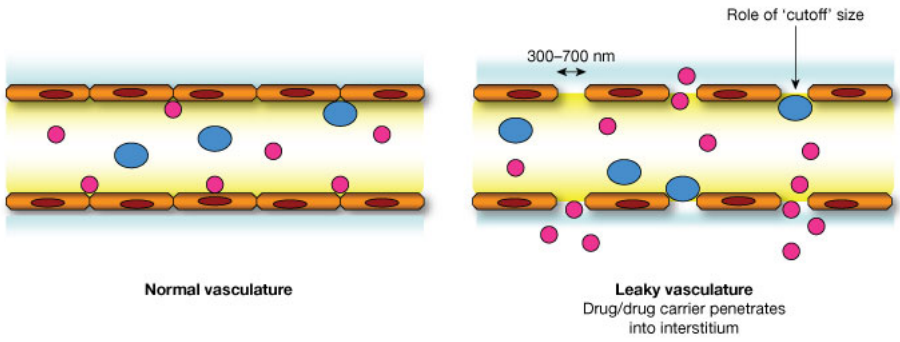

Figure 2.1: Schematic representation of the EPR-effect. Poor monolayer of the endothelial cells and impaired lymphatic drainage give rise to this phenomenon. Illustration adapted from [45]

2.1.3 The EPR effect - extravasation

Every tumor is different, so the properties described in the previous section are more prominent in some tumors than others. Regardless, the leaky vessels and poor lymphatic function give rise to the enhanced permeability and retention effect (EPR-effect). The EPR-effect is the most described and most promising property for the selective targeting of nanoparticles (NPs) to tumor sites [2].

The targeting effect is achieved as the NPs remain in the bloodstream where the blood vessels are normal, but would extravasate through the leaky vessels at the tumor site as shown in figure 2.1. The properties of the NPs that influence the EPR-effect include size, charge and surface characteristics.

2.1.4 NP characteristics

To overcome the physiological barriers and benefit from the EPR-effect described in the last sections, some general properties of the NP complex need to be investigated:

Size

Small particles (<10 nm) are efficiently removed from the blood stream by

the MPS [97] and this is usually also true for particles larger than 200 nm. Therefore, it is generally accepted that the optimal diameter for nanoparticle drug carriers is between 10 and 200 nm, but stealth techniques and altering other properties of the nanoparticles might influence this. Another consideration is the pore size, or the "cutoff" size, of the blood vessels, indicated in figure 2.1. As previously stated, the pore size can be as high as 2 μm, but the truth is that it is highly dependent on the different tumors and the microenvironment they are surrounded by [33].

Charge

Particles with highly charged surfaces are also removed efficiently from the circulation by MPS and the liver. The glomerular filtration in the kidneys are negatively charged and absorb positively charged molecules, but the cutoff size for filterable molecules is about 6-8 nm [6][18]. On the other hand, the extravasation across the blood vessels and in the tumors are increased for positively charged macromolecules [19].

Polarity

Hydrophobic molecules are associated with serum proteins and are recognized and metabolised by the liver [6]. Therefore, the nanoparticles should have a hydrophilic surface. This is often accomplished by pegylation as described in section 2.2.4.

2.2 Nanoparticles

2.2.1 Nanoparticles and medicine

The definition of a nanoparticle is a subject of controversy as some scientists emphasize on the size of the particles while other focus more on their properties. Either way, the term is used quite broadly these days and in this thesis all particles with a diameter in the nano-scale range (1-1000 nm) will be referred to as nanoparticles.

Particles in this size range are promising for many applications in medicine, because they can interact with cellular entities at their natural scale. In addition they have a high surface to mass ratio and it is usually quite easy to introduce new properties, or alter already existing properties. The research in this field have

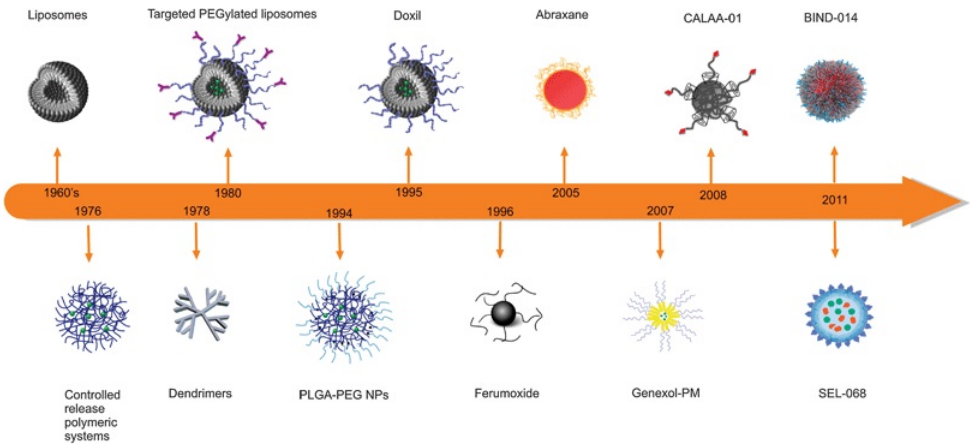

Figure 2.2: Timeline of developed NPs, which have been approved for human use or are undergoing clinical trials. Adapted from [40]

introduced a lot of different types of nanoparticles, where several distinct ones are presented in figure 2.2.

Nanoparticles have many uses in medicine and show promise in both diagnostic techniques and therapeutic techniques. Examples of therapy application in addition to drug delivery are:

- Nanotube and gold nanoparticle complexes accumulation in tumors and the use of infrared light to incinerate the cancer cells [104][51]
- NPs that reduce bleeding in trauma patients by activating the blood clotting mechanism [35]
- Buckyballs (spherical nanoparticles containing 60 carbon atoms) being able to trap free radicals generated during an allergic reaction and block inflammation [7].

Biosensing and imaging are also hot topics for nanoparticle research. Quantum dots are used for optical imaging, and superparamagnetic iron oxide nanoparticles are used as contrast agents in MRI [34]. Nanoparticles can be inherently contrast agents or carriers of different contrast agents. Multimodality is a popular term regarding the future development of nanoparticles. The intention is to incorporate several functionalities in a single particle. Research is also done in combining

nanoparticles, microbubbles and ultrasound for simultaneous diagnostics and enhanced therapeutic effect [62].

2.2.2 Poly (alkyl cyanoacrylate) nanoparticles

In the experimental work of this thesis, poly butylcyanoacrylate (PBCA) have been used. They are a subgroup of poly alkylcyanoacrylate (PACA). The idea of using PACA NPs as drug carriers emerged in the 1980s due to their size, structure, degradability, and drug sorptive properties [17]. The field of polymer nanoparticles (PNP) is quickly expanding and is thought to be useful in many different areas like electronics, photonics, pollution control, medicine and so on [25]. The number of publications cited on PNPs in an online database went from around 1500 in 2000 to more than 20000 in 2010, which tells us that this area of research is increasingly popular [76].

2.2.3 Synthesis of PNPs

Several methods are developed and successfully utilized to prepare PNPs. These methods can be separated in two main branches: 1) Prepare PNPs by dispersing preformed polymers and 2) Produce PNPs through the polymerization of monomers. An overview of these methods is given in figure 2.3.

The nanoparticles used in the experimental work of this thesis were made using the miniemulsion polymerization technique. When making particles with a hydrophobic core, a monomer of low water solubility, co-stabilizer, and the substance being encapsulated are mixed together in the oil-phase. The water-phase contains a surfactant and is usually acidic to have a surplus of protons. An initiator is usually also present and can be in both phases depending on its properties. The two phases are mixed and high shear forces are applied using a sonifier or a mechanical homogenizer, as shown in figure 2.4. Table 2.1 lists some advantages and disadvantages of this technique.

The most important substances in the miniemulsion technique are presented in the next four sections.

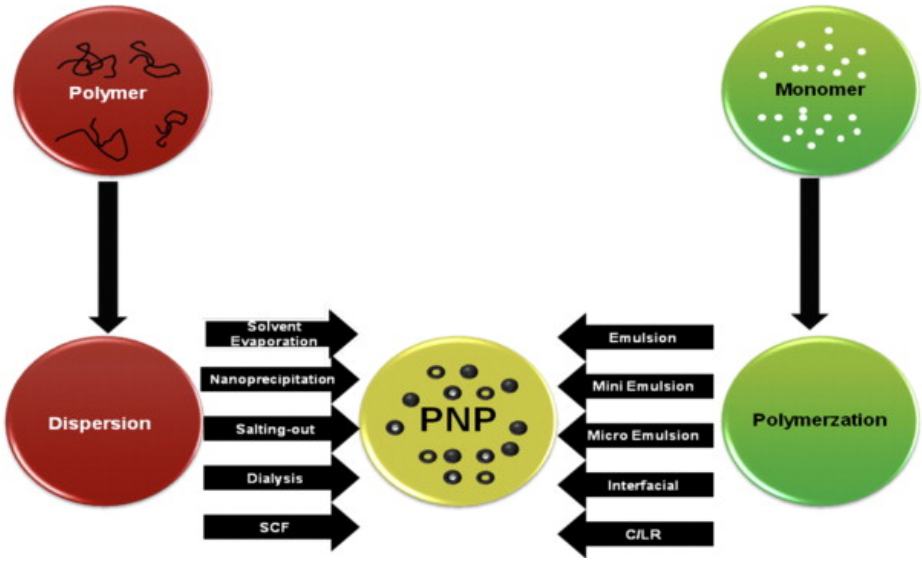

Figure 2.3: Overview of the different methods for preparing PNPs. Illustration adapted from [76]

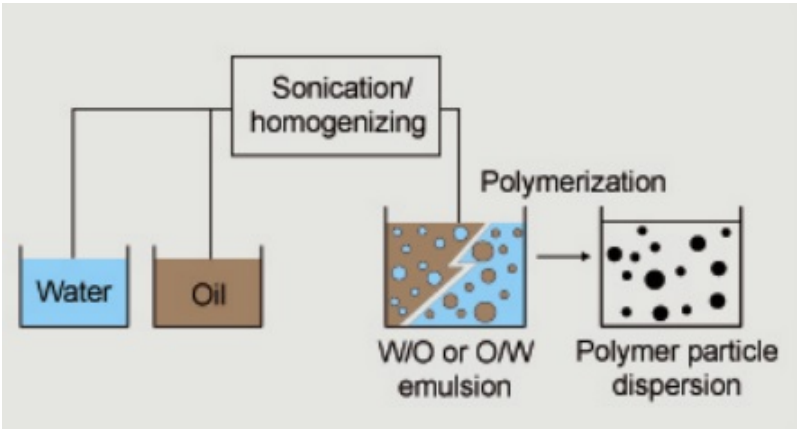

Figure 2.4: Schematic representation of miniemulsion polymerization process. Figure from Yrr Mørch, SINTEF Materials and Chemistry

Table 2.1: Pros and cons when preparing polymeric nanoparticles using the miniemulsion technique. Adapted from [101].

Advantages	Disadvantages
• One-step and low cost process	• High shear forces necessary
• Easy up-scaling to industrial scale	• Residual surfactant, monomer and/or stabilizer in the final product
• Compatible with a wide range of polymers	• Unwanted chemical reactions between active substance and monomer may occur before or during polymerization
• High loading with active substance, possible to encapsulate several substances in one step	• Lack of control of molecular weight and polydispersity of the polymer
• No need for further modification steps to add surface functionalization	

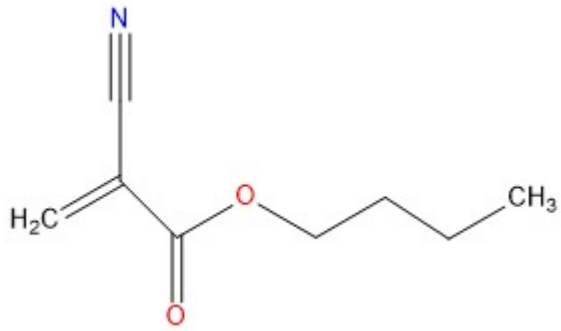

Figure 2.5: The chemical structure of butylcyanoacrylate.

Monomer

BCA (see figure 2.5) is the monomer in the particles used in the experimental work of this thesis. It is highly reactive to anions so in order to avoid premature polymerization, the emulsion has to be prepared in an acidic environment. The chain growth of BCA is illustrated in figure 2.6.

Initiator

A nucleophile, a molecule that donates an electron pair, initiates the anionic polymerization reaction. Many different nucleophiles can be used (like NaOH) and compounds with an amine group. Since BCA polymerizes easily, surfactants and PEG-chains can be used as initiators if they contain a reactive group and they are then added in the water-phase. A radical initiator in the oil-phase can also be used. To prevent premature polymerization it has to be non-reactive until it is triggered by heat.

Surfactant

The surfactant is a critical part in any emulsion polymerization. Its main role is to stabilize the emulsion by having a hydrophobic part inside the particle and a hydrophilic part protruding out, lowering the surface tension. One common surfactant is sodium dodecyl sulfate (SDS), see figure 2.7.

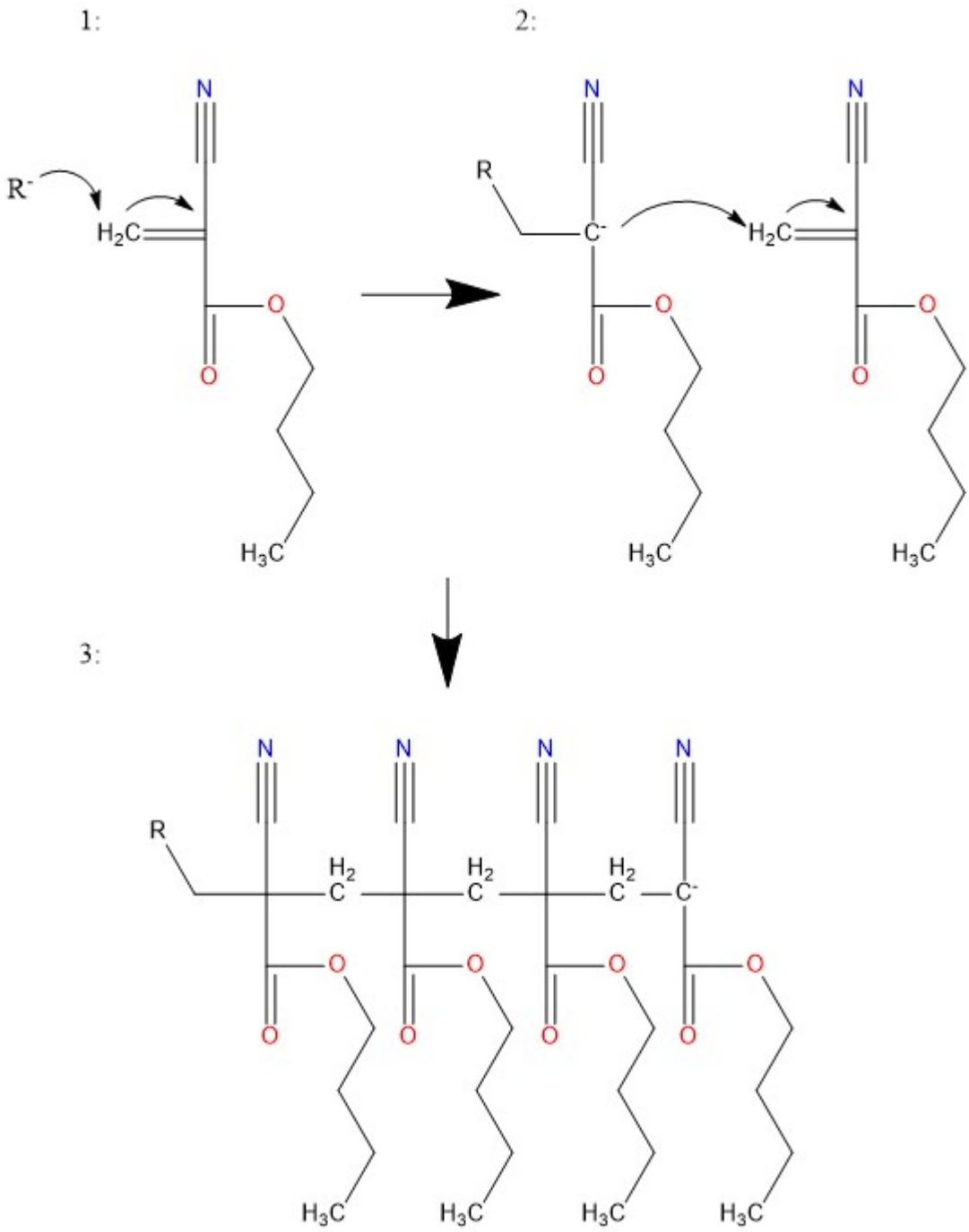

Figure 2.6: Polymerization of butyl cyanoacrylate: 1) An initiator with a free electron reacts with the CH_2 group. The central carbon atom that lost its double bond will then have a free electron. 2) The free electron in the central carbon atom can then react with the CH_2 group on another BCA monomer. 3) This reaction happens over and over and the end result is PBCA nanoparticles.

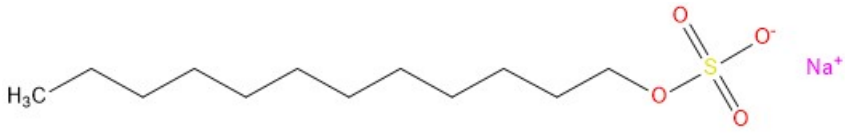

Figure 2.7: Chemical structure of SDS. It has a 12-carbon tail and a sulfate group, giving it the amphiphilic properties needed to be a surfactant.

Co-stabilizer

Molecules on the surface of PNPs are more unstable than the ones in the interior. This can cause the molecules to detach from the surface and stick to other nanoparticles. This phenomenon is called Ostwald ripening and causes larger particles to grow further in the expense of the smaller ones. It can also be explained by the fact that larger nanoparticles have lower surface area to volume ratio, thus being more energy favourable [91]. To prevent Ostwald ripening, a co-stabilizer is usually added in the oil-phase. By being very hydrophobic, the energy required for a molecule to detach from the surface increases to a point where it is very unlikely [59].

2.2.4 PEGylation

The human body is excellent at removing foreign objects. This is a problem, since a long circulation time is required for drug delivery processes. NPs without any kind of stealth strategy is removed from the blood circulation within minutes or at most a few hours by the mononuclear phagocyte system (MPS) [60]. Some strategies have been studied to work around this problem such as dextran conjugation [44], dendrimers [87], poly(ethylene oxide) [74], but PEGylation have shown to be most promising. PEGylation is the process of attaching polyethylene glycol (PEG) polymer chains to molecules. In addition to lengthen the circulation time, PEGylation may affect other properties of NPs, like uptake in cells and stability in different solutions.

There are three main properties of the PEG that impacts the circulation time of NPs: 1) the structure of PEG chains attached, 2) the number of PEG chains attached to the polypeptide and 3) the chemistry used to attach the PEG to the NPs [78]:

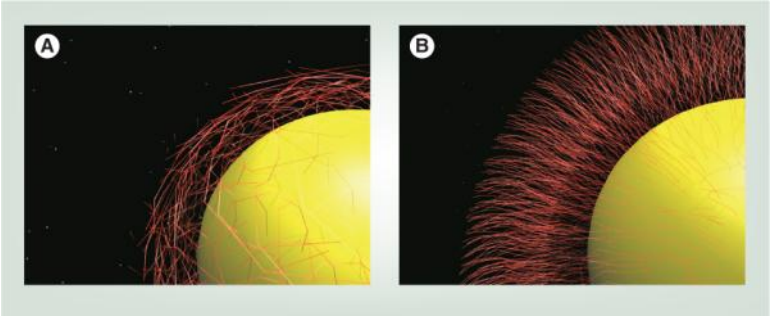

Figure 2.8: Illustration of a) the mushroom and b) the brush configuration of the PEG layer. Adapted from [38]

1. The basic structure of PEG is a linear or branched polyether with hydroxyl groups attached to each end:

   HO - (CH2$CH_2O)_n$ - CH_2CH_2 - OH,

   where n describes the length of the chain and is a crucial property of the PEG. The length is not easy to measure, so molecular weight (MW) is often used instead. Longer chains create greater steric hindrance, resulting in less recognition by macrophages and therefore lengthen the circulation time. The downside of long PEG chains is inhibition of cellular uptake and reduced active targeting properties [73]. Research indicates that a minimum MW of 2000 Da is required to achieve stealth characteristics [69].

2. The PEG layer is often described as being in the "brush" or the "mushroom" configuration, see figure 2.8. The mushroom arrangement appears when the PEG density is low, which results in the chains being closer to the surface. This increases the range of motion of each chain which increases the steric repulsion [86], but it may allow opsonin proteins to slip through the gaps and bind to the NP surface followed by excretion of the NP. With high PEG density, the chains extend from the surface and this is called the brush configuration. In this configuration there are no gaps in the PEG layer, but the mobility of the chains is very limited resulting in a decrease in steric repulsion. It is believed that the optimal PEG density is somewhere in between the mushroom and brush configurations [65].

3. Attaching the PEG to the surface of a PNP can be done both covalently and

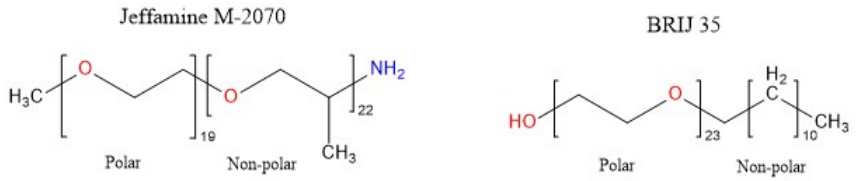

Figure 2.9: Chemical structure of Jeffamine M-2070 and BRIJ 35, showing the polar and non-polar parts.

noncovalently. In the miniemulsion polymerization technique, the PEG can act as an initiator and simultaneously be grafted to the particle [62]. Jeffamin M-2070 (see figure 2.9) is an example of such a PEG. The amin group on the hydrophobic part of the molecule initializes the polymerization and stays covalently attached to the PNP. An example of a PEG that is noncovalently attached to the PNP is BRIJ 35 (see figure 2.9). Because of its long aliphatic tail it attaches to the oil water interphase by hydrophobic interactions.

2.3 Cellular uptake of PNPs

There are different ways molecules and substances are transported through the plasma membrane of the cell. We can divide the mechanisms into passive movement across the membrane, which means that it does not consume energy, or active movement where the cell use energy to transport the substance. Small ions and molecules can enter through diffusion while some larger ones needs transmembrane protein channels to get through. Diffusion is always passive movement, while the use of tranmembrane protein channels can be both active and passive movement [30].

It is believed that nanoparticles can not pass through the cell membrane through diffusion or transmembrane protein channels due to their size. The last mechanism is the endocytosis. Endocytosis is the mechanism cells use to absorb larger molecules by engulfing them. Some of the best understood endocytic pathways are clathrin-mediated endocytosis (CME), caveolin mediated endocytosis, macropinocytosis and phagocytosis. Phagocytosis is not going to be described, since it mainly involves particles with a diameter of 2-3 μm. Although these are the primary ones, there are good evidence of other pathways [21]. Some molecules enter the cells exclusively through one pathway, but most can enter through several pathways.

An overview of some pathways can be seen in figure 2.10.

2.3.1 Internalization

Clathrin-mediated endocytosis

This is probably the best understood endocytosis. In CME, a ligand binds to a receptor on the cell surface and trigger a cascade of events[56]. First, the receptor attracts adaptor proteins (AP-2), before clathrin is recruited by the adapter protein. This leads to an invagination of the plasma membrane and with the help of the budding protein dynamin, it pinches off and forms a vesicle inside the cell. This vesicle now contains the ligand that was bound to its receptor and is coated with clathrin. The last steps are to uncoat the vesicle and recycle the receptors.

Endocytosis via Caveolae

Caveolae are rounded invaginations in the plasma membrane, typically 50-80 nm in diameter [72]. The endocytotic process is thought to start with the ligand binding to its receptor on the plasma membrane. After this initial step, the ligand diffuse laterally across the membrane until its trapped in caveolae. Then actin monomers are attracted to the caveolae and an actin patch is formed. As with CME, dynamin mediate the release of the vesicle from the membrane. Since caveolae is typically 50-80 nm one would think that this would also be the size limit the particle being internalized by this process. However, studies show that for particles with a diameter < 200 nm CME was involved, but with increasing particle size caveolae-mediated internalization became apparent. For particles of wit a diameter > 500 nm , endocytosis via caveolae became dominant [77].

Macropinocytosis

Some areas of the plasma membrane are highly ruffled. In these areas, the membrane can fold over to create vesicles. This uptake mechanism is not selective, meaning that one has not found any receptors which stimulates this process [90]. However, some proteins are heavily implicated in macropinocytosis like the kinase PAK1, PI3K, RAS and SRC [21].

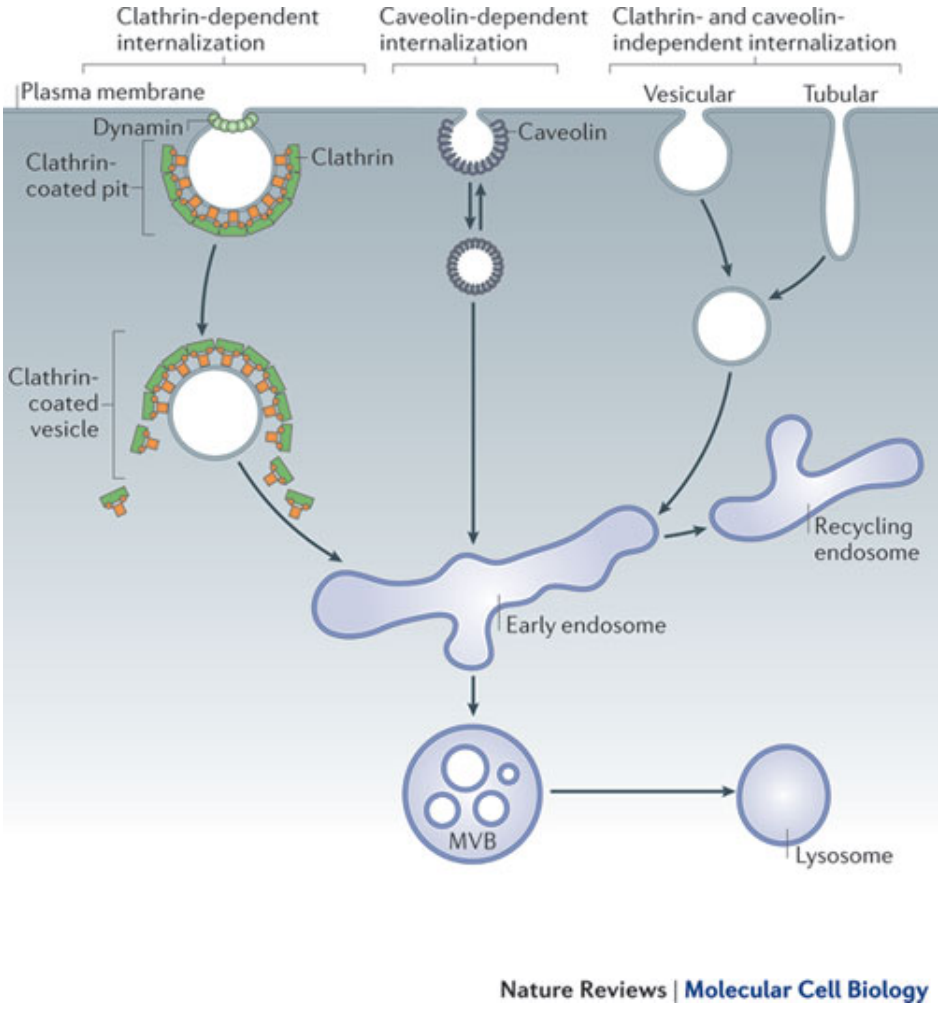

Figure 2.10: Illustration of clathrin-dependent, caveolin-dependent and clathrin- and caveolin-independent internalization of cargo. After internalization, the vesicle can fuse with other vesicles and become early endosomes. The cargo can then be recycled back to the surface or into other compartments like lysosomes. Throughout all these steps the cargo can also leak directly into cytosol. Illustration adapted from [55].

2.3.2 Intracellular trafficking

When a substance is internalized through endocytosis, the vesicle is thought to fuse with early endosomes. The early endosomes then mature to late endosomes (also known as MVB) before fusing with lysosomes, as shown in figure 2.10 [52]. The different compartments are distinguished by Rab GTPases and by the time it takes for endocytosed material to reach them [85].

Early endosomes

The primary function of early endosomes is sorting of the cargo. Receptors and membrane lipids are recycled back to the plasma membrane via recycling endosomes, while the internalized content proceeds to late endosomes [57]. Early endosomes are slightly acidic (pH 5.9-6.0) [41]. They represent a dynamic network of vesicles distributed throughout the cytoplasm. Their half-lives are cell and environment dependent, but a half-life of 5-10 minutes are normal [53].

Late endosomes

In the early endosomes, molecules are sorted into smaller vesicles that bud from the membrane and ends up in the lumen of the endosomes. This leads to the multivescular appearance of the late endosomes [29]. Late endosomes accumulate and increase the concentration of the internalized material. The pH is further decreased to around 5 [57] in order to break down its content.

Lysosomes

Late endosomes fuse with lysosomes, which can be described as the digestive system of the cell. They serve as the final destination for macromolecules before they are degraded. The lysosomes contain about 50 different acid hydrolase enzymes that are responsible for breaking down most substances [16].

2.3.3 Other outcomes for internalized substances

So far the pathway that leads endocytosed material to degradation in the lysosomes are described, but this pathway is not exclusive. The internalized material can escape this pathway [96], it can be transported to the trans-Golgi network or it can be brought back to the plasma membrane [27].

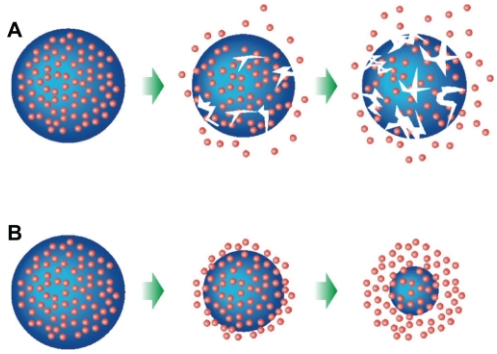

Figure 2.11: Two degradation mechanisms of nanospheres: A) bulk erosion, B) surface erosion [20]

2.4 Degradation of nanoparticles

Understanding the mechanisms for degradation are important to be able to control the rate of release of therapeutic agents. PACA NPs are so-called nanospheres where the therapeutic agents are dispersed throughout the polymeric matrix in contrast to nanocapsules where they are encapsulate in the core of the particles [28]. Two approaches to describe degradation are through bioerosion and the chemistry behind degradation.

2.4.1 Bioerosion

There are two forms of bioerosion of a nanosphere; surface erosion and bulk erosion, see figure 2.11.

These mechanisms are not exclusive and a combination of these is often seen [95]. The favoured mechanism depends on the size, degradation rate, density of polymer and the diffusion of water into the particle. Surface erosion happens when the rate of degradation exceeds the rate of water permeation into the bulk of the particle[95]. In PACA NPs the water permeation rate is slow and the degradation occurs mainly by surface erosion [94].

2.4.2 Chemistry behind degradation

PACA particles could be degraded through several chemical processes, as seen in figure 2.12.

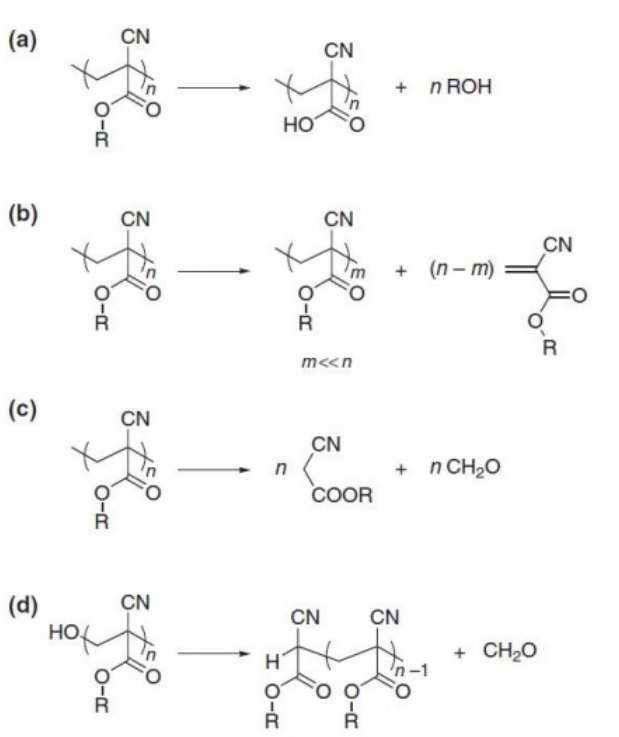

Figure 2.12: Different degradation possibilities for PACA particles. (a) hydrolysis of ester, resulting in poly(cyanoacrylic acid) and an alkylalcohol, (b) depolymerization followed by rapid re-polymerization, (c) inverse Knoevenagel reaction, (d) formaldehyde produced by hydrolysis of the α-hydroxyl function of the polymer chains. Illustration adopted from [8].

Wade and Leonard suggested in 1972 a degradation pathway involving ester-hydrolysis [98]. The reaction is initiated by a nucleophile (water or hydroxyl ion) attacking the carbon of the ester-group. This results in the water-soluble poly(2-cyanoacrylic acid) and a primary alcohol (butanol for PBCA). Esterases, enzymes that split esters, are found to catalyse the reaction.

Another pathway was suggested by Ryan and McCann in 1996 [81]. It involves the unzipping de-polymerization, accompanied by rapid polymerization of the polymer chain. The final polymer has lower molecular weight. The actual process is yet to be identified, probably since it happens so fast.

A third pathway was found back in 1966 by Leonard *et al.* [46]. They found that PACA degraded by hydrolytic scission of the polymer chain, also known as inverse Knoevenagel condensation. The end products in such a reaction are formaldehyde and alkyl cyanoacetate.

A fourth possibility for PACA degradation is the hydrolysis of the α-hydroxyl in the polymer chain.

The degradation pathway will vary depending on the conditions and surroundings. In a study it was found that PBCA particles had degraded 10 % after 30 days in pH 4, 70% after 30 days in pH 5.5 and 37 % after just 3.5 hours in pH 7.4 [8]. In cell medium the particles degraded slightly slower than in the pH 7.4 buffer.

2.5 Chemotherapeutic agents

At the beginning of the 20th century, scientists were able to transplant tumor models into animals which was a breakthrough in the development of chemotherapeutic agents (CA). Since then, a wide range of CAs have been developed. To understand how they work and why some can benefit from a PNP drug delivery system it is useful to know their properties and how they interact with our bodies and the cells.

2.5.1 Life cycle of a cell

Both normal cells and cancerous cells have to divide in order to replenish dead cells in the tissue they are part of. The cell division happens trough a series of events, called the cell cycle. It consists of four phases, as shown in figure 2.13.

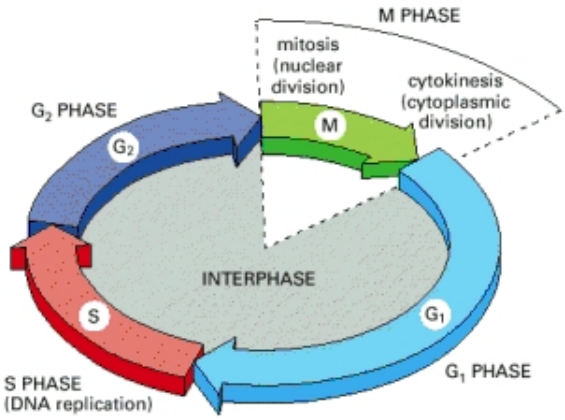

Figure 2.13: The four main phases of the cell cycle. Illustration adopted from [3].

G_1

G_1 is the first phase in the cell cycle. During G_1, the cells grow in size, form new organelles and synthesise more proteins. The time cells spend in G_1 varies a lot, from a few hours to years. If the extracellular conditions are unfavourable, cells may also enter a specialized resting state known as G_0. Some cells might stay in G_0 for the rest of their lifetime if they are fully differentiated or they have damaged DNA. When the extracellular conditions are favourable and signals to grow and divide are present, cells progress through a commitment point near the end of G_1 and starts to replicate the DNA [3].

S

In S-phase, cells duplicate their DNA. During synthesis, complex interactions between signalling and repair proteins act to prevent the process from going awry [5]. If something is wrong the cell is arrested until the problem is fixed. S-phase usually lasts for 8 hours, but it depends on the amount of DNA[16].

G_2

The gap between DNA synthesis and mitosis are called G_2. During this phase, the cell continue to grow and ensures that it is ready to enter mitosis and divide. The phase usually lasts about 4 hours[16].

M

The itosis (M) phase is when the cell divides and form two identical daughter cells. The cell stops its growth and focus the energy on the orderly division. M-phase lasts about an hour [16].

2.5.2 Taxanes

In 1971, the first taxane, Paclitaxel, was identified. Because of limited supply, the development was considerable delayed and it was first approved by the FDA for the treatment of ovarian cancer in 1992. Other well-known taxanes includes nab-paclitaxel and docetaxel. Docetaxel was approved as treatment for metastatic castration-resistant prostate cancer by the FDA in 2004[24].

Taxanes disrupt the microtubule function in the cells they infiltrate. Microtubules are tubular polymers of tubulin and are important in a number of cellular processes during the cell cycle. They play a particularly important role in mitosis and cell division where they build and then disassembles a specialized microtubule structure whose function is to separate the chromosome, figure 2.14 [50]. Taxanes interfere with the normal functions of microtubules by stabilizing them and thereby causes mitotic arrest [80]. In time this leads to cell death, but the actual apoptosis pathway are not fully understood and probably involves many different caspases and tumor proteins like p53 and p21 [37] [100].

2.5.3 Cabazitaxel

The taxane used in the experimental work of this thesis was Cabazitaxel. It was developed to treat castration-resistant prostate cancer in pasients that had developed resistance to docetaxel-based chemotherapy and was approved by the FDA in 2010 [1]. The mechanism of action is similar to that of its taxane predecessors, but some changes in the molecular structure (see figure 2.15) reduces its affinity for the P-glycoprotein efflux pump compared to docetaxel [66]. P-glycoprotein is an ATP-dependent efflux pump that pumps foreign substances out of cells. It is one of the main mechanism of docetaxel and other drug resistance in cells [99]. Cabazitaxel is lipophilic and insoluble in water [1].

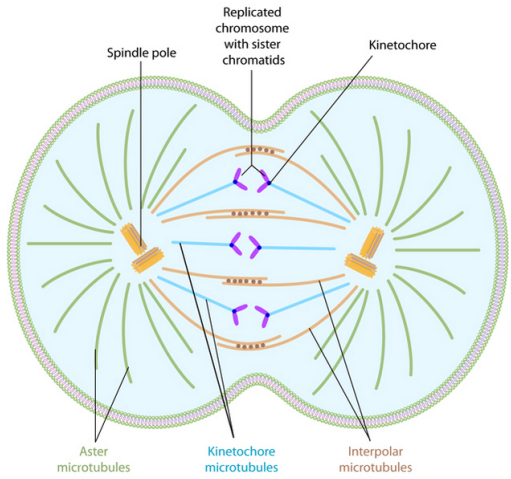

Figure 2.14: Several types of microtubules are active during mitosis. Illustration adopted from [67].

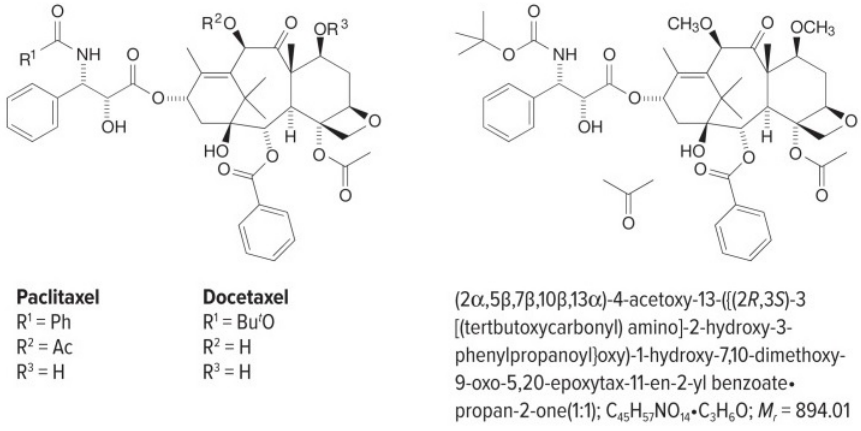

Figure 2.15: A comparison of the molecular structure of Paclitaxel, Docetaxel and Cabazitaxel. At the side chain, Cabazitaxel have replaced the hydroxyl groups of Docetaxel with methyl groups. Illustration adopted from [66].

2.5.4 Taxane formulations

Taxanes are inherently poorly soluble in water, therefore they can not be injected to patients in their pure form. Cremophor EL and polysorbate 80 have been the standard solvent system for taxanes, but negative side-effects including acute hypersensitivity reactions and peripheral neuropathy have been associated with these drugs [64]. This, in addition to the demand for targeted drug delivery in general, have lead the way to new formulations like Nab-paclitaxel, DJ-927, Larotaxel and PNPs [32] [93].

2.6 Experimental techniques

To interpret the results of the experimental work in this thesis it is crucial to have an understanding of the experimental techniques. These are explained in the following sections.

2.6.1 Fluorescence

Most experimental techniques used in this work make use of a property of some molecules called fluorescence. Fluorescence occurs when a substance emits light after having absorbed light or other electromagnetic radiation. The light emitted have longer wavelength, which means less energy due to loss of energy inside the substance. This is called stokes shift and is illustrated in figure 2.16. Fluorescence is a popular tool in biological research since you can image living organisms. In addition, fluorescent probes can be made to measure or image all sorts of biological events.

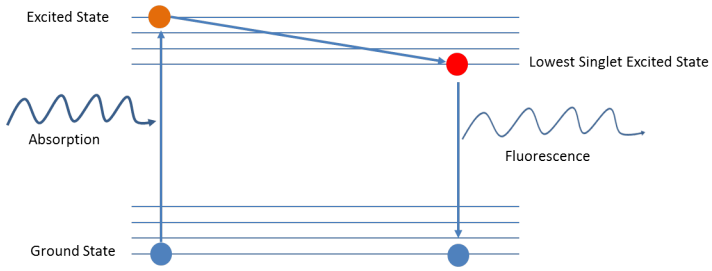

Figure 2.16: Energy level diagram of a molecule. The arrow between the orange and red dot indicates the stokes shift.

2.6.2 Confocal laser scanning microscopy

Confocal laser scanning microscopy (CLSM) is a very popular technique for imaging and analysing biological samples due to its high resolution, limited invasion of the sample and relatively easy sample preparation. The advantage of the CLSM compared to the traditional fluorescent microscope is the ability to block photons that are out of focus by the pinhole seen in figure 2.17. The pinhole is located in front of the detector and blocks photons originated from above or below the focal plane of the objective. Since it only detects photons from a limited area each time, the laser has to be scanned across the area you want an image from. The resolution depends on multiple parameters like the wavelength of the incident light, the characteristics of the objective, the settings of the scanning unit and the specimen. It is also limited by diffraction of light, which means that the best resolution is usually around 200 nm in the axial plane and around 500 nm in the lateral plane. There are also confocal variants of super-resolution like stimulate emission depletion microscopy (STED)[4]. Another feature of some CLSM microscopes are fluorescence lifetime imaging (FLIM). FLIM measures the lifetime of the excited state of the molecule; how long it takes from absorption of a photon until it is being emitted. This property varies with the local environment of the fluorophore [14].

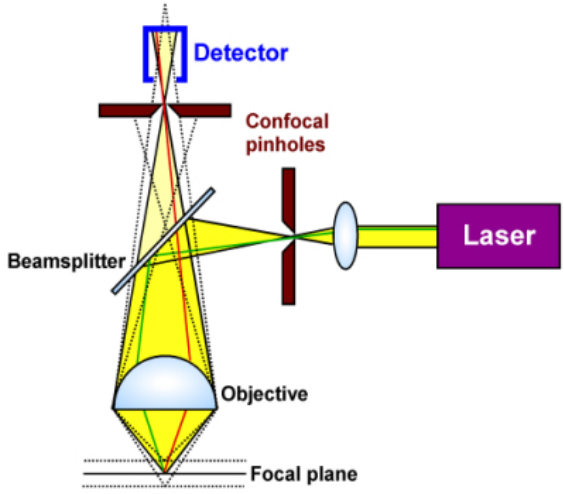

Figure 2.17: Light path in a confocal laser scanning microscope. Fluorescence not originated in the focal plane is blocked by the pinhole, thus achieving lower depth of field and higher depth resolution. Illustration adopted from [11].

2.6.3 Cell proliferation

Cell proliferation is the increase in cell number as a result of cell growth, cell division and cell death. It is increased in tumors and the purpose of chemotherapy is to decrease the proliferation. Cell proliferation is therefore often investigated in cytotoxicity studies. The three most used principles to study the proliferation in cell populations are: 1) Counting number of cells, 2) determine the total amount of DNA and 3) evaluate the metabolic activity. In each of these categories there are many different assays to use and deciding which method to use depends on many factors like equipment available, the experimental design and the expected outcome [103].

Metabolic activity

In the experimental work of this thesis, alamarBlue® (AB) was used to study proliferation of cell population. AB is a colorimetric assay that gives an indirect measure of metabolic activity in a cell population through oxidation-reduction. The active substance in AB is resazurin. Resazurin is a blue and nonfluorescent dye with an oxidation-reduction potential of +380 mV at pH 7 and 25℃ [75]. It acts as an electron acceptor and is reduced to the pink and highly fluorescent resorulfin. As Table 2.2 shows, AB is an intermediate in the final reduction of O_2 and cytochromes in the electron transport chain [50].

Table 2.2: Oxidation reduction potentials in the electron-transport system.

Reaction	Products	E^1o(mV), pH7.0, 25℃
$O_2 + 4H^+ + 4e^-$	$2H_2O$	+820
alamarBlue®$_{OX}$ + 2H + $2e^-$	alamarBlue®$_{PINK}$	+380
cytochromes$_{OX}$ + e^-	cytochromes$_{RED}$	+290 to +80
FMN + $2H^+$ + $2e^-$	$FMNH_2$	-210
FAD + $2H^+$ + $2e^-$	$FADH_2$	-220
NAD + $2H^+$+ + $2e^-$	NADH + H^+	-320
NADP + $2H^+$ + $2e^-$	NADPH + H^+	-320

The fluorescent intensities of the AB are often measured in a plate reader. A plate reader can usually excite fluorophores at different wavelengths and detect the fluorescence at different wavelengths. Sample reactions can be assayed in 6-1536

well plates.

2.6.4 Flow cytometry

Flow cytometry (FCM) was used in this work to study the impact of cabazitaxel encapsulated in PNPs on individual cells. In an FCM, cells in suspension are passing through an interrogation point one-by-one. The flow of particles is created by a jet stream of sheat fluid surrounding cells in suspension, a technique called hydrodynamic focusing [26]. At the interrogation point, monochromatic light intersects the cells and is scattered in all directions. The forward scatter light, light scattered along the same axis as the incident light, are detected. The intensity depends on the size of the cells. The side scatter, light detected orthogonal to the incident light, depends on the internal complexity of the cells [22]. In addition to the scattered light, different fluorescent dyes can be detected. Multiple fluorescent dyes can be detected using dichroic mirrors and multiple detectors, figure 2.18.

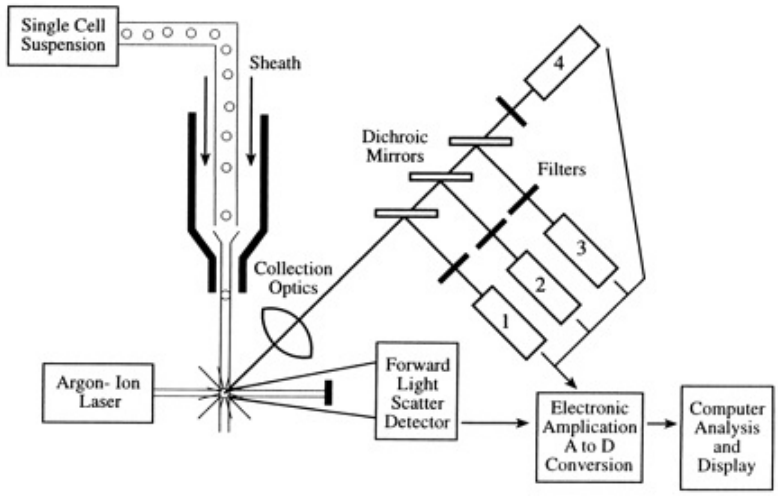

Figure 2.18: Schematic overview of a flow cytometer, showing the laminar flow of cells, forward scatter detector, side scatter detector (1) and multiple fluorescence emission detectors (2-4). Adopted from [10].

Flow cytometry is a quantitative method and one of its most important applications is DNA measurment. For DNA measurement and cell cycle analysis, it is necessary to stain or label the DNA with a fluorescent probe.

Chapter 3

Materials and methods

3.1 Cell cultivation

3.1.1 PC3

In the experimental work of this thesis, prostatic adenocarcinoma cells (PC3, American Type Culture Collection) were used for most of the experiments. These cells grow in a monolayer, attached to a surface. The growth is exponential and the number of cells doubles every 30 hours or so. The cells were cultivated in 75 cm^2 cell culturing flasks and were placed in an incubator with a temperature of 37°C and 5% CO_2. To keep the cells dividing, they require available space to grow on. To accomplish this, the cells were split every 3rd to 5th day after the last split.

The medium used for cell cultivation was Dulbecco's modified eagle medium (DMEM, Gibco Life Technologies) supplemented with 10% fetal bovine serum (PBS, Sigma Aldrich). Pencilin was used in the experiments involving 96-well plates and 6-well plates. Other solutions used in cultivation were sterile phosphate buffered saline (PBS, Sigma Aldrich) and 0,25% trypsin/0,02% EDTA (Sigma Aldrich).

For cell splitting a sterile bench was used and solutions were preheated to 37°C. First the old medium was removed. Then 5 mL PBS was added to wash away proteins that could inhibit trypsin to brake down anchor proteins of the cells. 3 mL trypsin was added and the flask was put in a room that held 37°C in 2-3 minutes. It is important not to let the trypsin work for too long, because it will attack vital compartments of the cells and lead to their deaths. When the cells had released

from the flask, 8 mL DMEM was added to inhibit trypsin. The solution was then added to a Falcon tube and centrifuged (Heraeus Megafuge 1.0) for 5 minutes at 1500 rpm. While this happened, the cell concentration was determined with the help of a cell counter (Countess, Invitrogen).

After centrifugation the supernatant was removed. The cells were then re-suspended to a concentration of 1 million/mL in DMEM. 1,5 million cells were transferred to a new cultivation flask and an extra 13,5 mL of DMEM was added to get a total volume of 15 mL. The rest of the cells were either used for experiments or thrown away.

3.1.2 HeLa

HeLa cells were cultured at 37℃ and 5% CO_2. Since they have a shorter lag phase than PC3 and have a more rapid growth, they were split more often. Otherwise they were treated the same way as PC3 cells. DMEM, supplemented with 10% FBS, 1% MEM Non-Essesntial Amino Acids (NEAA, Life technologies) and 0,5% L-Glutamin (Sigma Aldrich) was used as growth medium.

3.2 Nanoparticles

In this project poly butylcyanoacrylate (PBCA) particles were delivered by SINTEF materials and chemicals. Properties of these particles are listed in table 3.2.

3.2.1 Nile red

Encapsulated in the NPs was a modified Nile red dye (NR688)[42]. NR688 is highly lipophilic and therefore it does not leak out of the NP. It has excitation and emission maxima at 561 nm and 630 nm.

3.2.2 Cabazitaxel

SINTEF encapsulated Cabazitaxel (LC Laboratories) in the nanoparticles. The amount listed for BBB-30 in table 3.2 are theoretical value, but it was found that the encapsulation efficiency was close to 100%

3.3 Confocal laser scanning microscopy

3.3.1 Sample preparation

For CLSM, cells were placed in 8-well imaging plates (Ibidi). 10000 cells/ 300 μL were placed in each well three days before imaging. The plates were placed in the incubator to let the cells attach to the surface and grow. One day before imaging, CellLight® Lysosomes-GFP (CLL) (Lifetechnologies) was added at a concentration of 40 pieces per cell (ppc). The day of imaging, PBCA NPs were added at a concentration of 20 μg/mL and the samples were imaged.

3.3.2 Microscope

SP8 (Leica microsystems) was used for imaging. It was used with an incubation chamber that providing 37℃ and 5% CO_2 to give the cells the best possible conditions. A 63x1.4 oil based objective was used. CLL was excited with a white light laser at 488 nm and detected using a HyD-detector acquiring photons from 514 nm to 556 nm. NR668 was excited with a white light laser at 561 nm and detected with a photomultiplier tube (PMT) set up with a bandpass filter between 604 nm and 657 nm. In addition, a PMT detected the transmitted light.

3.4 Cell proliferation

3.4.1 Sample preparation

The cytotoxicity of cabazitaxel encapsulated in NPs was measured using alamarBlue® cell viability assay (Life technologies) and compared to cytotoxicity of cabazitaxel bound to DMSO (free drug). Three days prior to adding drug, 2500 PC3 cells/200μL medium were seeded in each well of a black 96 well plate with flat and clear bottom (Corning Incorporated). Since HeLa cells have a shorter lag phase, they were seeded one day before drug treatment at a density of 5000 cells/200μL in each well.

Both encapsulated drug and free drug was diluted in medium and added to the wells. Drug concentration in the experiments ranged from 0.025 ng/mL to 5000 ng/ml. Each concentration of free drug was matched with the same concentration of drug encapsulated in NP to compare the same concentrations. 4 replicas were used for each sample, including the control samples with only medium. Triton

X-100 was also used as a control in some experiments. After the addition of drug, the plates were put back into the incubator for the preferred duration. 72 hours incubation was usually preferred, but 16, 24, 48 and 96 hours were also tried.

On the day of measurement, the wells were rinsed three times with 200 μL medium. Then 110 μL AB diluted 10 times in medium was added to each well and the plates were put back into the incubator for 3 hours. Blank samples containing only medium and AB were also prepared in order to correct for background fluorescence from the medium.

3.4.2 Plate reader and data analysis

The fluorescence of AB was measured using a microplate reader (Tecan Group Ltd.). The measurements was done from the top with excitation and emission wavelengths of 550±9 nm and 590±20 respectively. An estimation of the percentage of viable cells was done with the equation below:

$$\text{Cell Viability}(\%) = \frac{FI_S - FI_B}{FI_{UC} - FI_B} \times 100, \tag{3.1}$$

where FI_S, FI_B and FI_{UC} are the fluorescence intensities from the treated wells, the background and the untreated controls respectively. The background fluorescence was not measured in the experiments done with HeLa cells and the following equation was therefore used to estimate cell viability for those:

$$\text{Cell Viability}(\%) = \frac{FI_S}{FI_{UC}} \times 100. \tag{3.2}$$

.

A dose response curve was fitted to these data using a 4 parameter logistic curve fit. The equation for this fitting is:

$$y = y_{min} + \frac{y_{max} - y_{min}}{1 + (x/EC_{50})^{-HillSlope}}, \tag{3.3}$$

.

where y_{min} and y_{max} are the minimum and maximum of the curve and were constrained to be equal or greater than 0 and smaller or equal to 100. EC_{50} denotes the half maximal effective concentration and $HillSlope$ is the largest absolute value of the slope of the curve. The coefficient of determination (R^2) and th P-values of each coefficient was used to discuss the goodness of the fitting. From the dose response curves, two measures of the samples cytotoxicity were obtained:

1. The median lethal dose (LD_{50}) refers to the dose required to kill half the members of a population after a specified time period. Low LD_{50} is indicative of increased toxicity. The value was determined by reading out at which concentration the cell viability was 50% in the graphs.

2. The half maximal effective concentration (EC_{50})) is the concentration of a drug which induces a response halfway between the baseline and the maximum after a specified duration and is commonly used as a measure of drug's potency.

3.5 Flow cytometry

FCM (Gallios, Beckman Coulter) was used to analyse DNA content and uptake of NPs in this thesis. DNA was stained with Hoechst 34580 (Sigma Aldrich), which has emission and excitation peaks at $\lambda = 392$ nm and $\lambda = 440$ nm respectively when bound to DNA.

3.5.1 Sample preparation

Three to five days prior to treatment, 200000 PC3 cells per 2 mL medium containing penicillin, were seeded in each well of a 6 well plate (Corning Incorporated). The cells were left in the incubator to attach and start growing. On the day of treatment, the growth medium was discarded and the test solutions were added in accordance with table 3.1.

Table 3.1: Schematic representation of the test solutions for DNA and uptake investigation with FCM.

Medium	0,4 μg/mL BBB-20 (Loaded with NR668 and 5% Cabazitaxel)	2 μg/mL BBB-20 (Loaded with NR668 and 5% Cabazitaxel)
2 μg/mL BBB-23 (Loaded with NR668)	0,02 μg/mL free cabazitaxel	0,1 μg/mL free cabazitaxel

On the day of measurement, each solution was moved to separate centrifuge tubes using pasteur pipettes. This step was performed to also measure non-

adherent cells (dead cells). Each well were then washed with 1 mL PBS, before trypsinization with 0,6 mL trypsin for 2-3 minutes at 37℃ was performed. Then, 3 mL medium was added to stop the trypsinization, before the solutions were put in their respective centrifuge tubes. The tubes were centrifuged at 1500 rpm for 5 minutes. The supernatant was removed using pasteur pipettes and the cells were re-suspended in 0,6 mL growth medium containing 40 μL Hoechst 34580 /mL medium. The tubes were then left for 20-30 minutes for the dye to bind to the DNA. Before running flow cytometry, the cells were transferred to FCM tubes.

3.5.2 Measurements and data analysis

Hoechst 34580 was excited using a laser at $\lambda = 405$ nm and detected at $\lambda = 450$ nm using a 50 nm bandpass filter. A laser at $\lambda = 561$ nm was used to excite NR668 which was detected at $\lambda = 620$ nm with a 30 nm bandpass filter. For every sample, approximately 30000 cells were measured.

Kaluza Analysis Software (Beckman Coulter) was used to analyse the measured data. The procedure for this was as follows:

1. A forward scatter (FS) versus side scatter (SS) diagram was used to gate out debris and aggregates as shown in figure 3.1a.

2. The cells gated from 1. were plotted with fluorescence intensity from DNA on the y-axis and FS on the x-axis. The relative fluorescent intensity for cells in G_1 was found and a gate including cells with DNA levels a little bit below the average for G_1 and some above twice this level was created. This is shown in figure 3.1b.

3. Cells gated by their size (1.) and by their DNA content (2.) were plotted with the number of cells on the y-axis and fluorescent intensity from DNA on the x-axis, as shown in figure 3.1c. From this plot, the percentage of cells in the G_1, S, and G_2+M was found. This step proved to be quite challenging and is discussed in detail in section 5.3.

4. The uptake of NPs was evaluated using the cells gated from (1.) and 2.) and plotted with number of cells along the y-axis and the fluorescent intensity from NR668 on a logarithmic x-axis.

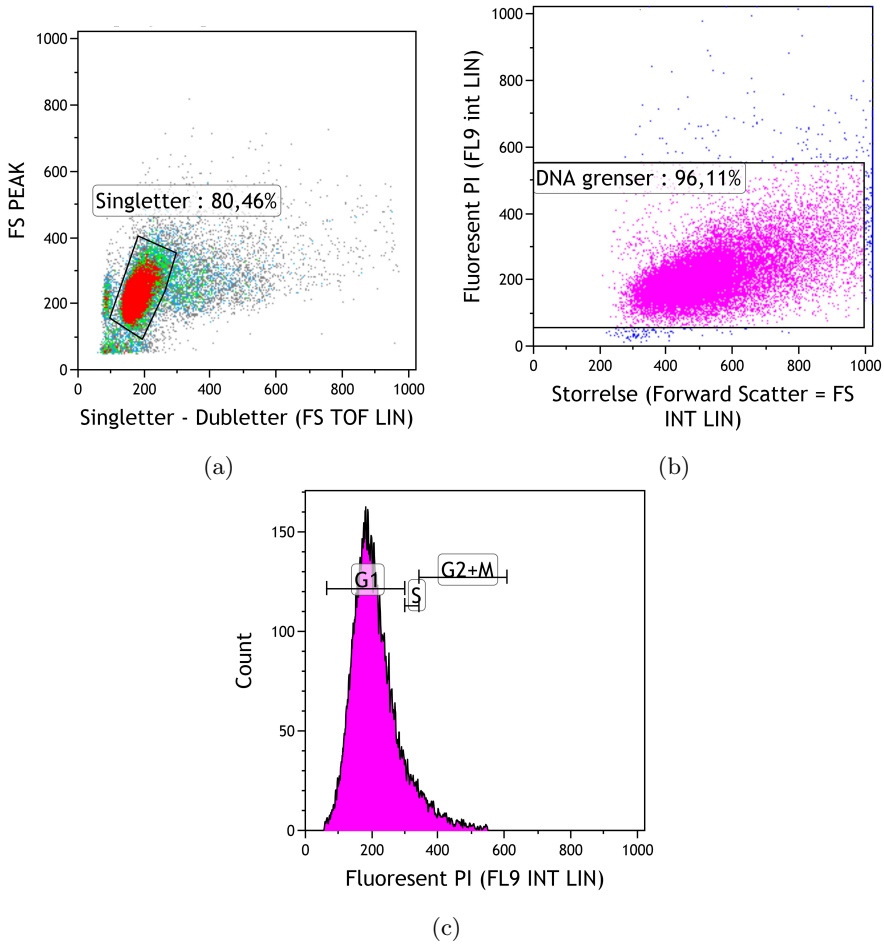

Figure 3.1: Some examples of the data analysing done in Kaluza. The sample in the examples are untreated cells that have been incubated for 12 hours. Figure (a) and (b) shows gating based on size and DNA respectively. Figure (c) is a plot with number of cells on the y-axis and fluorescent intensity from DNA om the x-axis. The cell cycle is indicated with G_1, S and G_2+M.

Table 3.2: List of NPs used.

Particle	Monomer	PEGylation	Size (nm)	Zeta potential (mV)	Encapsulated substance(% w/w)
Targ 120	BCA	Jeffamine M-2070 and Brij35	152	-4	NR668
BBB-20	BCA	Kolliphor HS15 and Pluronic F68	162	-6	4.4 cabazitaxel and 0.4 NR668
BBB-23	BCA	Kolliphor HS15 and Pluronic F68	150	-6	0.4 NR668
BBB-30	BCA	Kolliphor HS15 and Pluronic F68	165	-5	5 cabazitaxel
BBB-33B	BCA	Kolliphor HS15 and Pluronic F68	158	-4	-

Chapter 4

Results

The results are presented in three separate sections. The first is about intracellular localization of the NPs. The second section deals with the cytotoxicity of the chemotherapeutic agent cabazitaxel encapsulated in NPs and the comparison of free cabazitaxel and encapsulated cabazitaxel. Lastly, the results regarding the mechanism of encapsulated and free cabazitaxel and how it affects the cell cycle are presented.

4.1 Colocalization and intracellular route

By having knowledge of the intracellular route of the NPs, they can be further optimized to deliver drug at the target location. The intracellular localization can also say something about the uptake mechanisms as mentioned in the theory, section 2.3. To study the uptake mechanism and intracellular route of PBCA NPs, PC3 cells were stained with CellLight® Lysosomes-GFP and NPs (Targ-120) was added. CLSM was used to image the cells and look for colocalization of lysosomes and NPs. Some images and possible colocalization are presented in figure 4.1. The original plans was to also stain early endosomes and late endosomes to try to track the NPs in their internalization by the cells, but the uptake of PBCA NPs by PC3 cells was too low. The low uptake was confirmed by flow cytometry measurements done by colleagues (Unpublished results).

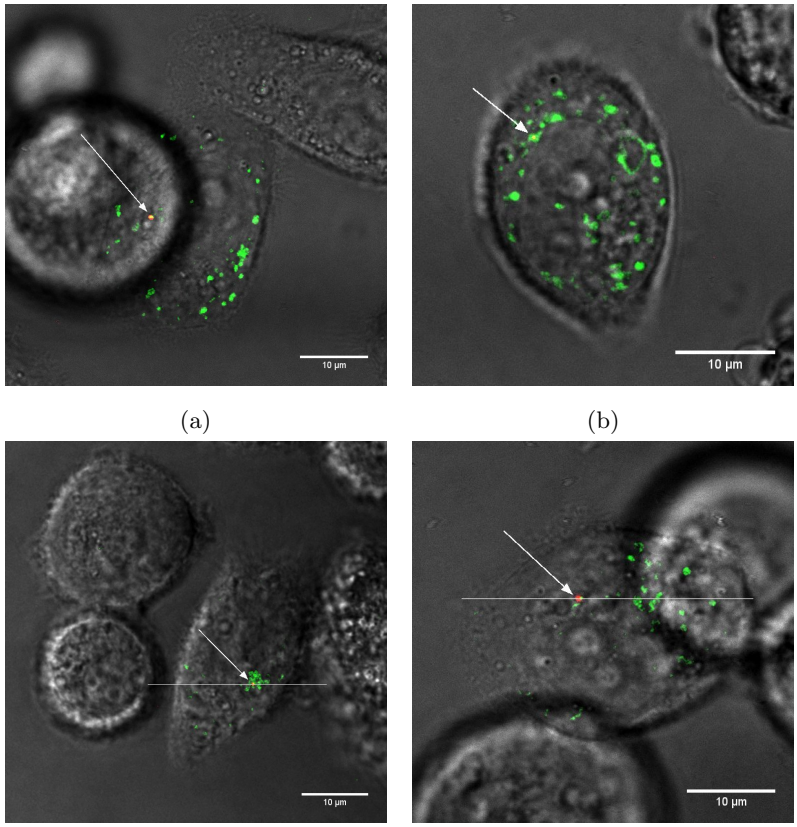

(a) (b)

(c) (d)

Figure 4.1: Cells that have been stained with CLL and incubated with NPs for approximately 3 hours. (c) and (d) also contains a line profile which is analysed in figure 4.2. Only some cells were transfected with CLL.

To verify the colocalization and examine the staining, line profile analysis was done and can be seen in figure 4.2. The peak in fluorescence intensity at the same positions indicates that the NPs actually was inside the lysosomes. In addition the data was assessed using a 3D modelling software as shown in figure 4.3.

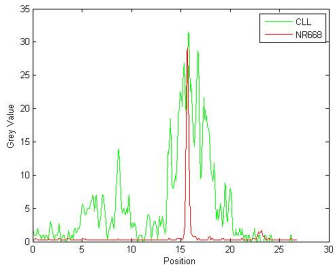

(a) Line profile of figure 4.1c.

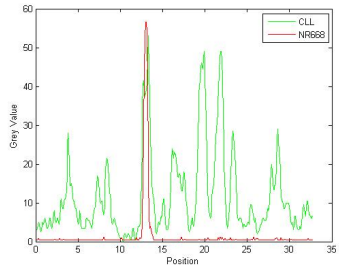

(b) Line profile of figure 4.1d.

Figure 4.2: Line profile to verify the colocalization and study the staining quality. In both (a) and (b), the two channels have a peak at the same position.

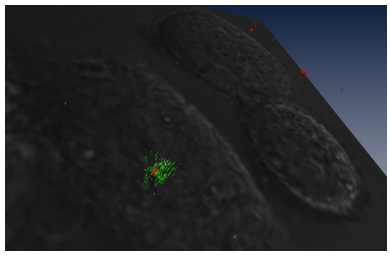

(a) 3D model from the Z-stack acquired of figure 4.1c.

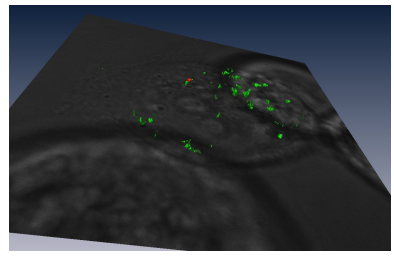

(b) 3D model from Z-stack acquired of figure 4.1d.

Figure 4.3: 3D models of the PC3 cells, acquired using Z-stack. The problem of low uptake can be clearly seen. In (a) most lysosome staining are concentrated in one area. Red spots are NPs while the green are the lysosome staining.

4.2 Cytotoxicity of encapsualted and free cabazitaxel

One of the main application on PNPs is drug delivery. Here, the use of PBCA NPs as drug carrier for cabazitaxel was studied in PC3 cells and HeLa cells using the cell viability assay alamarBlue® (AB). Figure 4.4a shows the resulting dose response curves for PC3 cells treated with encapsulated NPs and free drug for 72 hours. HeLa cells were chosen since they were readily available and have a faster cell growth than the PC3 cells. Cabazitaxel is known to inhibit cell division and it was

expected a higher cytotoxicity in the HeLa cells compared to the PC3 cells. Figure 4.4b shows the dose response curve for HeLa cells exposed to encapsulated drug and free drug for 72 hours and figure 4.4c shows the same for 48 hours exposure.

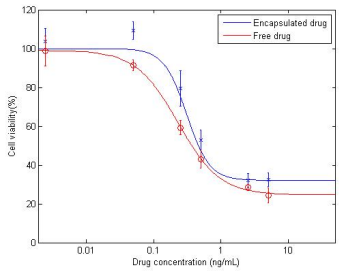

(a) PC3, 72 hours.

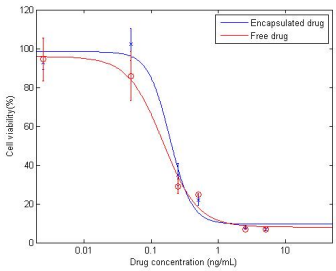

(b) HeLa, 72 hours

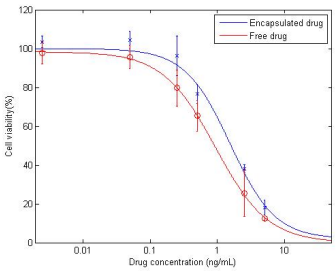

(c) HeLa, 48 hours

Figure 4.4: Dose response curves of PC3 and HeLa cells treated with cabazitaxel encapsulated in PBCA NPs and free cabazitaxel. The data points are an average of 4 identical samples of each dose with the standard deviation plotted as error bars. The x-axis displays increasing drug concentration on a logarithmic scale. More statistics and fitting are discussed in section 5.2.3.

In all three instances, the encapsulated drug requires a higher dose before making an impact on the cell viability compared to the free drug.

Table 4.1 summarises the LD_{50} and EC_{50} values. Lower values indicates higher cytotoxicity. The values are lower for HeLa cells compared to PC3 cells for the same exposure duration, as expected. And for the HeLa cells, the values are higher for shorter exposure time which is intuitive.

Table 4.1: LD_{50} and EC_{50} values summarized after testing the cytotoxicity of encapsulated and free cabazitaxel in PC3 cells and HeLa cells.

	PC3, 72 hours		HeLa, 72 hours		HeLa, 48 hours	
	NP	Free	NP	Free	NP	Free
LD_{50} (ng/mL)	0,462	0,368	0,203	0,158	1,588	0,903
EC_{50} (ng/mL)	0,314	0,227	0,188	0,147	1,540	0,931

4.3 Impact of cabazitaxel on the cell cycle

To further investigate cytotoxicity, the DNA content of PC3 cells treated with encapsulated cabazitaxel and free cabazitaxel was measured using flow cytometry. Figure 4.5 shows the difference in DNA content in untreated cells, cells treated with empty NPs, cells treated with drug-loaded NPs and cells treated with free drug, for 70 hours. It clearly shows that drug-loaded NPs and free drug have an impact on the DNA content and the corresponding cell cycle.

The six different treatments solutions (see table 3.1) were studied with 12, 22, 36, 46 and 70 hours incubation periods. Based on the cell distribution as a function of fluorescent intensity of DNA (as shown in figure 4.5) , cell cycle analysis was done and the resulting histograms are presented in figure 4.6. The drug seems to be making an impact already after 12 hours and the impact seems to be increasing with time.

The time dependency of encapsulated and free drug on the accumulation of cells in G2 and mitosis is presented in figure 4.7. It is a simple plot with few data points, but it looks like there is an increase of cells in G2 and mitosis with increased incubation durations which is expected. Depending on the drug release rate of the PBCA NPs, the less effect from encapsulated drug may be explained by it lagging behind the free drug.

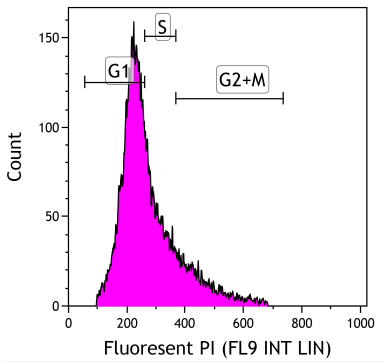

Gate	%Gated
All	100,00
G1	57,22
G2+M	16,58
S	26,18

(a) Untreated cells.

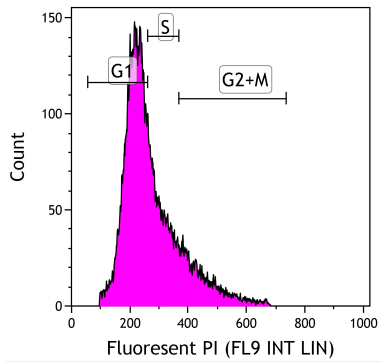

Gate	%Gated
All	100,00
G1	57,68
G2+M	16,40
S	25,88

(b) Cells treated with empty NPs.

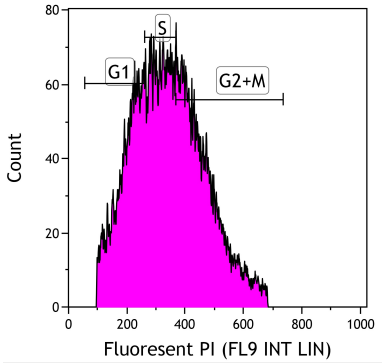

Gate	%Gated
All	100,00
G1	28,40
G2+M	40,89
S	30,63

(c) Cells treated with drug-loaded NPs.

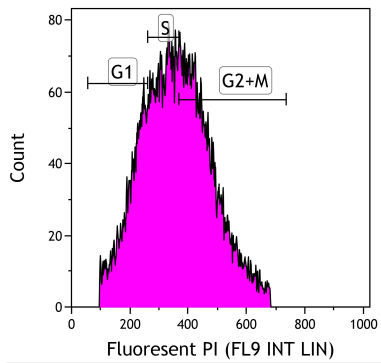

Gate	%Gated
All	100,00
G1	22,06
G2+M	46,69
S	31,19

(d) Cells treated with free drug.

Figure 4.5: Number of cells as a function of fluorescence intensity (DNA content) after 70 hours treatment. The DNA is stained with Hoecst 34580. (a) shows the distribution of untreated cells. (b) shows the distribution of cells treated with 2 μg/mL PBCA NPs, loaded with NR668 (BBB-23). (c) shows the distibution of cells treated with 0,4 μg/mL PBCA NPs, loaded with 5% cabazitaxel and NR668 (BBB-20). The effective concentration of encapsulate cabazitaxel is 20 ng/mL. (d) shows the distribution of cells treated with 20 ng/mL free cabazitaxel. In all instances, the corresponding phases of the cell cycle is marked.

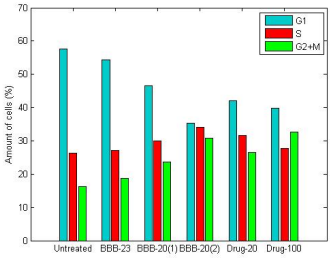

(a) 12 hours treatment.

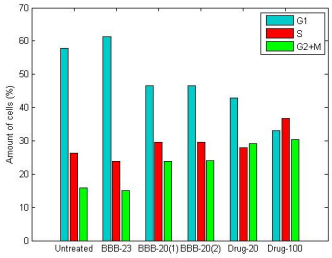

(b) 22 hours tratment.

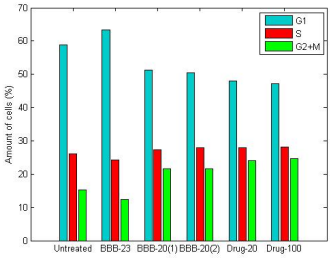

(c) 36 hours treatment.

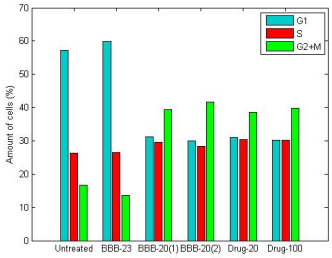

(d) 46 hours treatment.

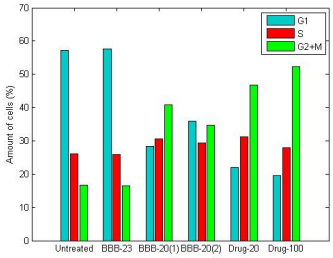

(e) 70 hours treatment.

Figure 4.6: Cell cycle distributions for the treatment duration stated. BBB-23 is particles loaded with NR668 and the concentration used was 2 μg/mL. BBB-20 is particles loaded with cabazitaxel and NR668. The concentrations used for these particles were (1) 0,4 μg/mL and (2) 2 μg/mL, which corresponds to 20 ng/mL and 100 ng/mL of cabazitaxel. Drug-20 and Drug-100 is cells treated with free cabazitaxel with a concentration of 20 ng/mL and 100 ng/mL respectively.

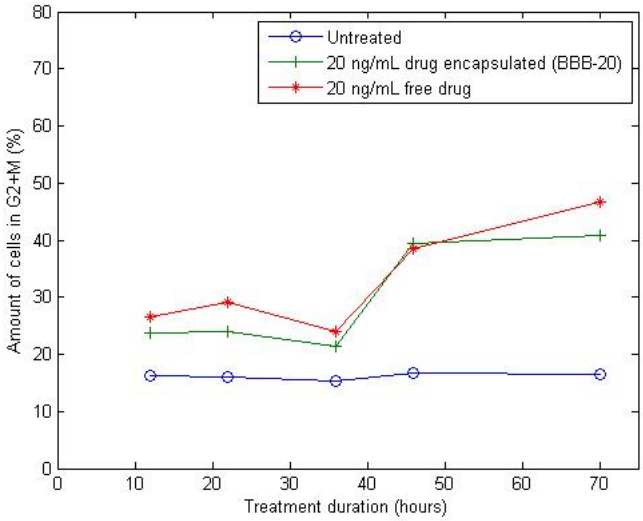

Figure 4.7: Time dependence of the accumulation of cells in the G2+mitosis phase of the cell cycle.

Chapter 5

Discussion

This project is divided in two separate parts. First the intracellular localization of PBCA NPs was assessed. The experiment set-up and the result of this is discussed in section 5.1. The second part was to investigate the effect of cabazitaxel encapsulated in PBCA NPs. Two different approaches were used to investigate the effect and they are discussed in section 5.2 and section 5.3. In section 5.4 some genereal considerations and the impact of these results will be discussed and some further work will be suggested.

5.1 Intracellular localization

For drug delivery purposes it is essential to know the intracellular pathway of the NPs to be able to control the release rate and the destination of the drug. Previous work done by Einar Sulheim showed that PBCA NPs were endocytosed primarily through clathrin-mediated endocytosis and that the uptake was low in PC3 cells [89]. The normal route of substances going through this uptake mechanism is early endosomes and late endosomes before entering lysosomes. This can be a problem in drug delivery since lysosomes are known to degrade many therapeutic agents. In addition, lysosomes have a pH around 4,5 and 5,0 [58], a pH which the PBCA NPs show little to no degredation [9]. Sulheims work indicated that PBCA NPs were able to escape the lysosomes and this is also reported by other groups [49] [15].

5.1.1 Lysosome staining

The experiments done in the first part were a continuation of my project thesis where I stained lysosomes with Lysotracker® blue and looked for colocalization between lysosomes and NPs [47]. In that work, very little colocalization was found between NPs and lysosomes, but it was suggested that it was due to the experimental set-up. Lysotracker® blue had to be excited by a multiphoton laser which could cause a poor alignment with the laser that excited the NR668. In addition, this dye is attracted to acidic organelles in the cells since it is a weak base linked to a fluorophore, which might not stain the lysosomes if the acidic environment is changed by the NPs.

In this work, CLL was used to stain lysosomes. CLL uses a transfection technique where the cells expresses a fusion construct of Lamp1 and green fluorescent protein (GFP) after transfection. Lamp1 is a transmembrane protein that resides primarily across lysosomal membranes [12]. Therefore it does not depend on the acidic property of lysosomes. GFP have excitation maxima at 488 nm and could be excited with the same white light laser as excites NR668, which should remove most of the alignment problems seen when using Lysotracker.

5.1.2 Colocalization of NPs and the endocytic organelles

The initial objective was to study the NPs way through early endosomes, late endosomes and lysosomes. It was decided to start with the colocalization between lysosomes and PBCA NPs, since the early and late endosomes have shorter half-lives and lysosomes are the end point of the endocytic pathway. The first experiments was done by transfecting the cells with CLL as normal and adding the NPs just before imaging. But in these experiments, no uptake of NPs was seen. The uptake of NPs are energy dependent and also known to be dependent on the culturing conditions of the cells. Therefore the ability of the incubation chamber on the microscope to hold 37°Cand 5% CO_2 is of great importance and might be the reason why no uptake was seen.

Figure 4.1 shows colocalization between PBCA NPs and lysosomes. In these experiments, the cells were incubated with PBCA NPs for 3 hours in the incubation chamber before the imaging was started. Most of the PBCA NPs found inside cells were associated with lysosomes which is in accordance with the literature [82].

Due to the low uptake of these PBCA NPs in PC3 cells and the short half-lives of

late and early endosomes, as described in section 2.3.1 it was decided not to pursue colocalization between NPs and these organelles. Despite that, these colocalization results support the theory of PNPs taken up by the endocytic pathway, leading to lysosomes.

5.1.3 Uptake of PBCA NPs encapsulated with cabazitaxel and NR668

While doing cytotoxic measurement in the flow cytometer, the uptake of the NPs were simultaneously measured by exciting and detecting the NR668. It was found that the low concentration of NPs used when doing cytotoxic studies was too low to actually get some good uptake results, but the measurement showed that unhealthy cells may produce autofluorescence at this excitation and emission wavelength. In Appendix A, the increase in fluorescence signal from cells treated with free drug compared to untreated cells can be seen. The fluorescence signal is further increased for cells treated with BBB-20 and BBB-23, which is expected since they are loaded with NR668. For all the treated samples, the signal is increasing with time compared to the untreated sample. This indicate that the cells produce autofluorescence at this wavelength when they are in a toxic environment. While this increase in fluorescence is quite low compared to the increase seen when doing uptake studies of NPs at a concentration of 20 μg/mL [89], it should be considered when doing uptake studies for longer incubation periods.

5.2 Cytotoxicity effect of drug using proliferation assay

One of the main reasons for studying intracellular localization is to predict the destiny of drug encapsulated in the NPs. The knowledge of the uptake, the degradation and the cytotoxicity of the PBCA NPs was sufficient to move on to study the effect of an encapsulated drug. The drug chosen was cabazitaxel, which are described in section 2.5.3. It is a novel drug used to treat men with advanced prostate cancer that has progressed after treatment with other anti-cancer medicines. It is very hydrophobic which makes it easy to encapsulate in the NPs. In addition, taxanes are quite stable at pH 4-5, so even though the particles might end up in the lysosomes for degradation, the drug can work if it can escape the lysosomes [92].

AlamarBlue® (AB) was used to investigate the cytotoxcicity of the encapsulated drug.

5.2.1 AlamarBlue® assay

The protocol made for measuring cytotoxicity with AB was based on the manufacturer recommendations and a protocol found in a previous master thesis [48] [101]. In the initial experiments, the cells seemed to be growing mostly towards the edges of each well in the 96 well plates. In an online discussion forum it was recommended to move the plates backward and forward, then right to left a couple of times to get an even spread of cells after seeding. This technique improved the spread of cells in the experiments done in this thesis. In addition, the edge effect, known to altering the rate of cell growth at the edges of microplates due to evaporation, was taken into account by not using the outer wells in the final experiments [36].

5.2.2 Initial experiments

In the initial experiments, drug concentrations ranging from 5 ng/mL to 5000 ng/mL (corresponding NPs concentrations are 100 ng/mL to 100 μg/mL) were tested. These were based on IC_{50} values reported in literature ranging from 2,5 ng/mL to 500 ng/mL [43] [71] and the previous studies of cytotoxicity of empty NPs showing that they were non-toxic at a concentration up to 20 μg/mL for 3 hours treatment and 24 hours treatment [101].

Results from one of the initial experiments are included in Appendix B. It was found that the impact of drug did not vary much at concentrations from 25 ng/mL to 1000 ng/mL and lower concentrations had to be measured to produce dose response curves. In addition, it was found that the concentration of 20 μg/mL with empty PBCA NPs was toxic to the cells for longer incubation periods.

5.2.3 Statistical analysis

The dose response curves in figure 4.4 was fitted using Sigmaplot. The R^2 and P-values are listed in table 5.1. The R^2 values are all above 0,98 which indicates that the data fits the curves quite well. On the other hand, some P-values are above the common alpha level of 0.05 (marked red in table 5.1), which indicates that the coefficients are not statistically significant. This may be due to poor experimental design, wrong model for the data or too few data. In this case, particularly figure

4.4b and figure 4.4c, the statistics of the curve fitting would be better if there was included some higher doses. The curves would be the very similar since the minimum value are close to zero anyway. Due to the not optimal statistics, I will emphasise more on the trends and comparisons from these results, than the actual numbers.

Table 5.1

	PC3, 72 hours		HeLa, 72 hours		HeLa, 48 hours	
	NP	Free	NP	Free	NP	Free
R^2	0,9809	0,9992	0,9858	0,9895	0,9858	0,9996
P_{min}	0,0284	0,0027	0,2260	0,2273	0,9554	1,0000
P_{max}	0,0030	0,0020	0,0049	0,0044	0,0028	0,0001
P_{EC50}	0,0322	0,0036	0,0691	0,0550	0,2765	0,0123
$P_{HillSlope}$	0,1631	0,0076	0,2890	0,0695	0,1533	0,0063

5.2.4 PC3 versus HeLa

As described in the theory, taxanes inhibit cell division by stabilizing the microtubules. Since the HeLa cells have a more rapid cell cycle than PC3 cells, the drug was expected to have a greater cytotoxicity in the HeLa cells. The lower LD_{50} and EC_{50} for HeLa cells shown in table 4.1 indicates that this is true. Taxanes are also known to induce adoptosis though two different pathways [61]. HeLa cells are reported to die within 48-72 hours after taxane treatment, while PC3 cells go though a slow cell death pathway [39] [13]. This can explain why the cell viability stabilizes around 35% for PC3 cells and around 10% for HeLa cells as can be seen in figure 4.4.

5.2.5 Encapsulated drug and free drug

From the dose response curves it seems like the encapsulated drug requires a higher concentration than the free drug to get an effect. The observation can be linked to the drug being less potent when encapsulated in the nanoparticles compared to being bound to DMSO, or it can be related to the release rate of the drug in the nanoparticles. By comparing HeLa cells after 48 hours incubation and 72 hours incubation it looks like the encapsulated and free drug response curves are getting

closer as time passes. The LD_{50} and EC_{50} values are also more similar for the 72 hours incubation as presented in table 4.1, which indicates that the degradation of PBCA NPs may take at least some hours. Studies on non-drug loaded PBCA NPs found that they were considerably degraded after 24 hours [89]. Cabazitaxel is very hydrophobic and may stabilize the NPs and decrease the degradation rate. From these experiments it is difficult to say something about the potency of encapsulated versus free drug, but the results indicates that the cytotoxicity of cabazitaxel is not inhibited by being encapsulated in PBCA NPs.

5.3 Cytotoxicity of encapsulated drug using cell cycle distribution

Since the cell cycle is the main target of taxanes it was decided to investigate the impact of encapsulated and free drug through cell cycle analysis. This was done by measuring the DNA content in PC3 cells treated with encapsulated and free cabazitaxel in a flow cytometer.

5.3.1 Experimental set-up

Hoechst 34580 was chosen to stain the DNA, since the excitation and emission wavelengths does not interfere with the excitation and emission wavelengths of NR668 and it was readily available. In the first experiment, the recommended concentration of 5 μg/mL gave very little fluorescence. A range of concentrations were then tested and it was found that 40 μg/mL provided decent fluorescent signal. This concentration is 8 times higher than the manufacturer recommends. The reason such high concentration had to be used was most likely due to the excitation maximum of Hoechst 34580 being around $\lambda = 380$ nm, while the excitation laser used in the flow cytometer was at $\lambda = 405$ nm. At this wavelength, the absorption is only 15% of maximum [83].

5.3.2 Prediction of cell cycle distribution

From the measurement of DNA content, the number of cells in each phase of the cell cycle were estimated. To accomplish this, assumptions of the duration of G_1, S and G_2+M were made. S-phase and G_2+M was set to be 8 hours and 5 hours respectively, which is common for rapidly proliferating human cells [16]. The

doubling time for PC3 cells was found to be 30,5 hours by a colleague, which yield 17,5 hours for the G_1 phase. In other words it was assumed that for untreated cells, the amount of cells in G_1, S and G_2+M were 57,4%, 26,2% and 16,4% respectively. For each incubation period, gates for the cell cycle phases was made with this in mind, as can be seen in figure 3.1c. The gates were then copied to the data containing cells treated with drugs and the amount of cells in the different phases of the cell cycle was determined. The assumptions made of the cell cycle phases are doubtful and caution should be exercised when using the amount of cells in the different phases given in this thesis.

5.3.3 Impact of encapsulated drug on the cell cycle

In an ideal cell cycle experiment based on DNA content, there would be two peaks: one for cells in G_1 and one for cells in G_2+M with twice the DNA and twice the fluorescent intensity. In between the two peaks, the cells synthesizing DNA would be. Figure 4.5 shows the cell cycle distribution for untreated cells and cells treated with encapsulated and free drug. Despite not having two peaks, it is obvious that both encapsulated drug and free drug make an impact on the cell cycle distribution. An increase in the DNA content is clearly seen.

To investigate if there was a delayed response for the encapsulated drug compared to the free drug, five different incubation durations were tested ranging from 12 hours to 70 hours. Depending on the release rate of the encapsulated drug, the accumulation of cells in G_2+M would be delayed compared to the free drug. The result, presented in figure 4.6 and figure 4.7 indicate that the response for encapsulated drug are lagging behind, but the measurements and analysis are not accurate enough to say anything about the actual release rate.

5.4 General considerations and further work

The experimental work and analyses done in this thesis shows some of the potential of polymeric nanoparticles as drug delivery carriers. SINTEF found it easy to encapsulate cabazitaxel in the NPs and the effect of encapsulated drug was similar to the free drug in these *in vitro* studies.

Going from here to *in vivo* studies and finally being used as medicine is still quite fare ahead. One of the main challenges for the PNPs is to obtain sufficient

circulation times *in vivo* due to the MPS [68]. Another challenge is the poor intratumoral distribution of the particles due to the elevated interstitial fluid pressure and the size of the macromolecules [69]. The shielding of the PNPs are still being optimized and ultrasound have been found to facilitate the extravasation and tumor uptake of the NPs [23]

5.4.1 Further work

Based on the work in this thesis I have following suggestions for future directions:

- The result from colocalization investigations supports the hypothesis that PNPs are taken up by endocytosis and going through the endocytic machinery, but the underlying mechanism are not fully described yet. Gathering this knowledge is beneficial for further optimization. I recommend finding a cell line with higher uptake of the NPs or using NPs that have a higher uptake in the PC3 cells. Since the uptake is dependent on the culturing conditions of the cells, the incubation chamber on the microscope should be checked by using external thermometer and CO_2 sensor. If the uptake is sufficient one might be able to track particles as they are being internalized.

- In the experimental work of this thesis it was found that cabazitaxel encapsulated in PBCA NPs had an effect similar to cabazitaxel bound to DMSO, but the release mechanisms and the rate of release was only partially studied. It would be interesting to study cabazitaxel in more stable particles like PIHCA or POCA. PIHCA NPs have a slower degradation rate than PBCA and a delayed response would be expected. POCA particles show very little degradation even after a week [89]. By investigating the cytotoxicity of cabazitaxel encapsulated in POCA NPs one could argument if the drug are leaking out of the NPs or not.

- One the path to clinical use of PNPs as drug delivery carriers it is necessary with *in vivo* studies. When accumulation of non-drug loaded PNPs in tumors of mice is believed to be sufficient for treatment, one should start investigating the effect of drug-loaded PNPs in animals.

Chapter 6

Conclusion

Intracellular localization of PBCA NPs in PC3 cells have been evaluated using CLSM. Lysosomes were stained with CellLight® Lysosomes-GFP and the PBCA NPs were loaded with NR668. Colocalization between the lysosomes and the PBCA NPs was studied and the following conclusion was made:

- The PBCA NPs were colocalized with lysosomes, which strengthens the belief that endocytosis is the uptake mechanism of these cells.

The cytotoxicity of the novel taxane, cabazitaxel encapsulated in PBCA NPs was investigated in PC3 cells and HeLa cells through cell proliferation and cell cycle distribution. AlamarBlue® cell viability assay was used to study the cell proliferation, while Hoechst DNA staining and flow cytometry was used to evaluate the cell cycle. The following conclusions were made:

- Cabazitaxel encapsulated in PBCA NPs had a cytotoxic effect on both PC3 cells and HeLa cells, which suggests that the NPs or the released drug is able to escape the lysosomes.
- The cytotoxic effect of encapsulated cabazitaxel was similar to cabazitaxel bound to DMSO. It was indicated that the response from encapsulated cabazitaxel was lagging behind in time compared to cabazitaxel bound to DMSO.

Bibliography

[1] Afroz Abidi. Cabazitaxel: A novel taxane for metastatic castration-resistant prostate cancer-current implications and future prospects. *Journal of Pharmacology & Pharmacotherapeutics*, 4(4):230–237, 2013.

[2] Sarbari Acharya and Sanjeeb K. Sahoo. PLGA nanoparticles containing various anticancer agents and tumour delivery by EPR effect. *Advanced Drug Delivery Reviews*, 63(3):170–183, March 2011.

[3] Bruce Alberts, Alexander Johnson, Julian Lewis, Martin Raff, Keith Roberts, and Peter Walter. An overview of the cell cycle. 2002.

[4] Carlos Alonso. An overview of stimulated emission depletion (STED) microscopy and applications. *Journal of Biomolecular Techniques : JBT*, 24(Suppl):S4, May 2013.

[5] J. M. Bailis, D. D. Luche, T. Hunter, and S. L. Forsburg. Minichromosome maintenance proteins interact with checkpoint and recombination proteins to promote s-phase genome stability. *Molecular and Cellular Biology*, 28(5):1724–1738, March 2008.

[6] Thomas M. Behr, Robert M. Sharkey, Malik E. Juweid, Rosalyn D. Blumenthal, Robert M. Dunn, Gary L. Griffiths, Hans-J. Bair, Friedrich G. Wolf, Wolfgang S. Becker, and David M. Goldenberg. Reduction of the renal uptake of radiolabeled monoclonal antibody fragments by cationic amino acids and their derivatives. *Cancer Research*, 55(17):3825–3834, September 1995.

[7] Hayley Birch. Buckyballs could help fight allergies. *Nature News*, July 2007.

[8] A. Bøe. *Degradation and Stability of PBCA and POCA Nanoparticles*. Master thesis, NTNU, 2013.

[9] Andreas Gagnat Bøe. Degradation and stability of PBCA and POCA nanoparticles. *105*, 2013.

[10] Michael Brown and Carl Wittwer. Flow cytometry: Principles and clinical applications in hematology. *Clinical Chemistry*, 46(8):1221–1229, August 2000.

[11] D. Bucher. A practical guide for fluorescent confocal microscopy — the marder lab.

[12] S. R. Carlsson and M. Fukuda. Structure of human lysosomal membrane glycoprotein 1. assignment of disulfide bonds and visualization of its domain arrangement. *The Journal of Biological Chemistry*, 264(34):20526–20531, December 1989.

[13] Giuliana Cassinelli, Cinzia Lanzi, Rosanna Supino, Graziella Pratesi, Valentina Zuco, Diletta Laccabue, Giuditta Cuccuru, Ezio Bombardelli, and Franco Zunino. Cellular bases of the antitumor activity of the novel taxane IDN 5109 (BAY59-8862) on hormone-refractory prostate cancer. *Clinical Cancer Research*, 8(8):2647–2654, August 2002.

[14] Leng-Chun Chen, William R. Lloyd, Ching-Wei Chang, Dhruv Sud, and Mary-Ann Mycek. Fluorescence lifetime imaging microscopy for quantitative biological imaging. *Methods in Cell Biology*, 114:457–488, 2013.

[15] Zhiqin Chu, Silu Zhang, Bokai Zhang, Chunyuan Zhang, Chia-Yi Fang, Ivan Rehor, Petr Cigler, Huan-Cheng Chang, Ge Lin, Renbao Liu, and Quan Li. Unambiguous observation of shape effects on cellular fate of nanoparticles. *Scientific Reports*, 4, March 2014.

[16] Geoffrey M. Cooper. *The Cell*. Sinauer Associates, 2nd edition, 2000.

[17] P. Couvreur, B. Kante, V. Lenaerts, V. Scailteur, M. Roland, and P. Speiser. Tissue distribution of antitumor drugs associated with polyalkylcyanoacrylate nanoparticles. *Journal of Pharmaceutical Sciences*, 69(2):199–202, February 1980.

[18] W. M. Deen, B. Satvat, and J. M. Jamieson. Theoretical model for glomerular filtration of charged solutes. *The American Journal of Physiology*, 238(2):F126–139, February 1980.

[19] M Dellian, F Yuan, V S Trubetskoy, V P Torchilin, and R K Jain. Vascular permeability in a human tumour xenograft: molecular charge dependence. *British Journal of Cancer*, 82(9):1513–1518, May 2000.

[20] R Dinarvand, N Sepehri, S Manoochehri, H Rouhani, and F Atyabi. Polylactide-co-glycolide nanoparticles for controlled delivery of anticancer agents. *International Journal of Nanomedicine*, 6:877–895, 2011.

[21] Gary J. Doherty and Harvey T. McMahon. Mechanisms of endocytosis. *Annual Review of Biochemistry*, 78:857–902, 2009.

[22] Ryan Duggan. Basic parameters measured by a flow cytometer: What is scattered light and absolute fluorescence?, 2013.

[23] Siv Eggen. *Ultrasound in Imaging and Delivery of Nanomedicine in Cancer Tissue*. NTNU, 2015.

[24] FDA. Approval for docetaxel, http://www.cancer.gov/about-cancer/treatment/drugs/fda-docetaxel.

[25] Kurt E. Geckeler and Hiroyuki Nishide, editors. *Advanced Nanomaterials*. Wiley-VCH Verlag GmbH & Co. KGaA, Weinheim, Germany, December 2009.

[26] Joel P. Golden, Gusphyl A. Justin, Mansoor Nasir, and Frances S. Ligler. Hydrodynamic focusing – a versatile tool. *Analytical and bioanalytical chemistry*, 402(1):325–335, January 2012.

[27] Barth D. Grant and Julie G. Donaldson. Pathways and mechanisms of endocytic recycling. *Nature reviews. Molecular cell biology*, 10(9):597–608, September 2009.

[28] Gareth Griffiths, Bo Nyström, Suraj B. Sable, and Gopal K. Khuller. Nanobead-based interventions for the treatment and prevention of tuberculosis. *Nature Reviews Microbiology*, 8(11):827–834, November 2010.

[29] Jean Gruenberg and Harald Stenmark. The biogenesis of multivesicular endosomes. *Nature Reviews Molecular Cell Biology*, 5(4):317–323, April 2004.

[30] Jeff Hardin, Gregory Bertoni, Lewis J. Kleinsmith, and Wayne M. Becker. *Becker's world of the cell*. Benjamin Cummings, Boston, 8th ed edition, 2012.

[31] Carl-Henrik Heldin, Kristofer Rubin, Kristian Pietras, and Arne Östman. High interstitial fluid pressure — an obstacle in cancer therapy. *Nature Reviews Cancer*, 4(10):806–813, October 2004.

[32] K. L. Hennenfent and R. Govindan. Novel formulations of taxanes: a review. old wine in a new bottle? *Annals of Oncology*, 17(5):735–749, May 2006.

[33] Susan K. Hobbs, Wayne L. Monsky, Fan Yuan, W. Gregory Roberts, Linda Griffith, Vladimir P. Torchilin, and Rakesh K. Jain. Regulation of transport pathways in tumor vessels: Role of tumor type and microenvironment. *Proceedings of the National Academy of Sciences of the United States of America*, 95(8):4607–4612, April 1998.

[34] Yong-Min Huh, Young-wook Jun, Ho-Taek Song, Sungjun Kim, Jin-sil Choi, Jae-Hyun Lee, Sarah Yoon, Kyung-sup Kim, Jeon-Soo Shin, Jin-Suck Suh, and Jinwoo Cheon. In vivo magnetic resonance detection of cancer by using multifunctional magnetic nanocrystals. *Journal of the American Chemical Society*, 127(35):12387–12391, September 2005.

[35] Anna N Ilinskaya and Marina A Dobrovolskaia. Nanoparticles and the blood coagulation system. part i: benefits of nanotechnology. *Nanomedicine*, 8(5):773–784, May 2013.

[36] Kevin Jaquith. Three ways to reduce microplate edge effect, http://www.wellplate.com/three-ways-reduce-microplate-edge-effect/.

[37] Michael Jelínek, Kamila Balušíková, Martina Schmiedlová, Vlasta Němcová-Fürstová, Jan Šrámek, Jitka Stančíková, Ilaria Zanardi, Iwao Ojima, and Jan Kovář. The role of individual caspases in cell death induction by taxanes in breast cancer cells. *Cancer Cell International*, 15(1):8, 2015.

[38] Jesse V Jokerst, Tatsiana Lobovkina, Richard N Zare, and Sanjiv S Gambhir. Nanoparticle PEGylation for imaging and therapy. *Nanomedicine (London, England)*, 6(4):715–728, June 2011.

[39] M. A. Jordan, K. Wendell, S. Gardiner, W. B. Derry, H. Copp, and L. Wilson. Mitotic block induced in HeLa cells by low concentrations of paclitaxel (taxol) results in abnormal mitotic exit and apoptotic cell death. *Cancer Research*, 56(4):816–825, February 1996.

[40] Nazila Kamaly, Zeyu Xiao, Pedro M. Valencia, Aleksandar F. Radovic-Moreno, and Omid C. Farokhzad. Targeted polymeric therapeutic nanoparticles: design, development and clinical translation. *Chemical Society Reviews*, 41(7):2971, 2012.

[41] Ikramy A. Khalil, Kentaro Kogure, Hidetaka Akita, and Hideyoshi Harashima. Uptake pathways and subsequent intracellular trafficking in nonviral gene delivery. *Pharmacological Reviews*, 58(1):32–45, March 2006.

[42] Andrey S. Klymchenko, Emilie Roger, Nicolas Anton, Halina Anton, Ievgen Shulov, Julien Vermot, Yves Mely, and Thierry F. Vandamme. Highly lipophilic fluorescent dyes in nano-emulsions: towards bright non-leaking nano-droplets. *RSC Advances*, 2(31):11876–11886, November 2012.

[43] Charles A. Kunos, Tammy Stefan, and James W. Jacobberger. Cabazitaxel-induced stabilization of microtubules enhances radiosensitivity in ovarian cancer cells. *Frontiers in Oncology*, 3, September 2013.

[44] L M Lacava, Z G Lacava, M F Da Silva, O Silva, S B Chaves, R B Azevedo, F Pelegrini, C Gansau, N Buske, D Sabolovic, and P C Morais. Magnetic resonance of a dextran-coated magnetic fluid intravenously administered in mice. *Biophysical Journal*, 80(5):2483–2486, May 2001.

[45] David Lembo and Roberta Cavalli. Nanoparticulate delivery systems for antiviral drugs. *Antiviral Chemistry and Chemotherapy*, 21(2):53–70, 2010.

[46] Fred Leonard, R. K. Kulkarni, George Brandes, Joshua Nelson, and John J. Cameron. Synthesis and degradation of poly (alkyl α-cyanoacrylates). *Journal of Applied Polymer Science*, 10(2):259–272, 1966.

[47] Kjetil Viste Levik. Intracellular localization of POCA and PBCA nanoparticle. *Project thesis dep.physics NTNU*, 2015.

[48] Life Technologies. Manual alamarBlue® assay.

[49] Peifeng Liu, Yanming Sun, Qi Wang, Ying Sun, He Li, and Yourong Duan. Intracellular trafficking and cellular uptake mechanism of mPEG-PLGA-PLL and mPEG-PLGA-PLL-gal nanoparticles for targeted delivery to hepatomas. *Biomaterials*, 35(2):760–770, January 2014.

[50] Harvey Lodish, Arnold Berk, S. Lawrence Zipursky, Paul Matsudaira, David Baltimore, and James Darnell. *Molecular Cell Biology*. W. H. Freeman, 4th edition, 2000.

[51] E. Y. Lukianova-Hleb, E. Y. Hanna, J. H. Hafner, and D. O. Lapotko. Tunable plasmonic nanobubbles for cell theranostics. *Nanotechnology*, 21(8):085102, February 2010.

[52] J. P. Luzio, B. A. Rous, N. A. Bright, P. R. Pryor, B. M. Mullock, and R. C. Piper. Lysosome-endosome fusion and lysosome biogenesis. *Journal of Cell Science*, 113 (Pt 9):1515–1524, May 2000.

[53] Frederick R. Maxfield and Timothy E. McGraw. Endocytic recycling. *Nature Reviews Molecular Cell Biology*, 5(2):121–132, February 2004.

[54] Donald M. McDonald and Peter Baluk. Significance of blood vessel leakiness in cancer. *Cancer Research*, 62(18):5381–5385, September 2002.

[55] Harvey T. McMahon and Emmanuel Boucrot. Molecular mechanism and physiological functions of clathrin-mediated endocytosis. *Nature Reviews Molecular Cell Biology*, 12(8):517–533, August 2011.

[56] PS McPherson, B. Ritter, and B. Wendland. Clathrin-mediated endocytosis. *Landes Bioscience*, 2000.

[57] Ira Mellman. Endocytosis and molecular sorting. *Annual Review of Cell and Developmental Biology*, 12(1):575–625, 1996.

[58] Joseph A. Mindell. Lysosomal acidification mechanisms. *Annual Review of Physiology*, 74(1):69–86, 2012.

[59] Vikas Mittal. *Miniemulsion Polymerization Technology*. John Wiley & Sons, January 2011.

[60] S. Moein Moghimi, A. Christy Hunter, and J. Clifford Murray. Long-circulating and target-specific nanoparticles: Theory to practice. *Pharmacological Reviews*, 53(2):283–318, June 2001.

[61] P. J. Moos and F. A. Fitzpatrick. Taxanes propagate apoptosis via two cell populations with distinctive cytological and molecular traits. *Cell Growth & Differentiation: The Molecular Biology Journal of the American Association for Cancer Research*, 9(8):687–697, August 1998.

[62] Ýrr Mørch, Rune Hansen, Sigrid Berg, Andreas K. O. Åslund, Wilhelm R. Glomm, Siv Eggen, Ruth Schmid, Heidi Johnsen, Stephan Kubowicz, Sofie Snipstad, Einar Sulheim, Sjoerd Hak, Gurvinder Singh, Birgitte H. McDonagh, Hans Blom, Catharina de Lange Davies, and Per M. Stenstad. Nanoparticle-stabilized microbubbles for multimodal imaging and drug delivery. *Contrast Media & Molecular Imaging*, April 2015.

[63] Gera Neufeld and Ofra Kessler. Pro-angiogenic cytokines and their role in tumor angiogenesis. *Cancer Metastasis Reviews*, 25(3):373–385, September 2006.

[64] P. Z. New, C. E. Jackson, D. Rinaldi, H. Burris, and R. J. Barohn. Peripheral neuropathy secondary to docetaxel (taxotere). *Neurology*, 46(1):108–111, January 1996.

[65] Arthur R. Nicholas, Matthew J. Scott, Nigel I. Kennedy, and Malcolm N. Jones. Effect of grafted polyethylene glycol (PEG) on the size, encapsulation efficiency and permeability of vesicles. *Biochimica et Biophysica Acta (BBA) - Biomembranes*, 1463(1):167–178, January 2000.

[66] Ginah Nightingale and Jae Ryu. Cabazitaxel (jevtana). *Pharmacy and Therapeutics*, 37(8):440–448, August 2012.

[67] C. M. O'Conner and J. U. Adams. *Essentials of Cell Biology.* 2010.

[68] M. Ogris, P. Steinlein, S. Carotta, S. Brunner, and E. Wagner. DNA/polyethylenimine transfection particles: influence of ligands, polymer size, and PEGylation on internalization and gene expression. *AAPS pharmSci*, 3(3):E21, 2001.

[69] Donald E. Owens III and Nicholas A. Peppas. Opsonization, biodistribution, and pharmacokinetics of polymeric nanoparticles. *International Journal of Pharmaceutics*, 307(1):93–102, 2006.

[70] Timothy P. Padera, Ananth Kadambi, Emmanuelle di Tomaso, Carla Mouta Carreira, Edward B. Brown, Yves Boucher, Noah C. Choi, Douglas Mathisen, John Wain, Eugene J. Mark, Lance L. Munn, and Rakesh K. Jain. Lymphatic metastasis in the absence of functional intratumor lymphatics. *Science (New York, N.Y.)*, 296(5574):1883–1886, June 2002.

[71] Vaishali Pannu, Prasanthi Karna, Hari Krishna Sajja, Deep Shukla, and Ritu Aneja. Synergistic antimicrotubule therapy for prostate cancer. *Biochemical pharmacology*, 81(4):478–487, February 2011.

[72] Lucas Pelkmans and Ari Helenius. Endocytosis via caveolae. *Traffic (Copenhagen, Denmark)*, 3(5):311–320, May 2002.

[73] Daniela Pozzi, Valentina Colapicchioni, Giulio Caracciolo, Susy Piovesana, Anna Laura Capriotti, Sara Palchetti, Stefania De Grossi, Anna Riccioli, Heinz Amenitsch, and Aldo Laganà. Effect of polyethyleneglycol (PEG) chain length on the bio-nano-interactions between PEGylated lipid nanoparticles and biological fluids: from nanostructure to uptake in cancer cells. *Nanoscale*, 6(5):2782–2792, March 2014.

[74] Fabiana Quaglia, Luisanna Ostacolo, Giuseppe De Rosa, Maria Immacolata La Rotonda, Massimo Ammendola, Giuseppe Nese, Giovanni Maglio, Rosario Palumbo, and Christine Vauthier. Nanoscopic core-shell drug carriers made of amphiphilic triblock and star-diblock copolymers. *International Journal of Pharmaceutics*, 324(1):56–66, October 2006.

[75] Sephra N. Rampersad. Multiple applications of alamar blue as an indicator of metabolic function and cellular health in cell viability bioassays. *Sensors (Basel, Switzerland)*, 12(9):12347–12360, September 2012.

[76] J. Prasad Rao and Kurt E. Geckeler. Polymer nanoparticles: Preparation techniques and size-control parameters. *Progress in Polymer Science*, 36(7):887–913, July 2011.

[77] Joanna Rejman, Volker Oberle, Inge S. Zuhorn, and Dick Hoekstra. Size-dependent internalization of particles via the pathways of clathrin- and caveolae-mediated endocytosis. *The Biochemical Journal*, 377(Pt 1):159–169, January 2004.

[78] M. J. Roberts, M. D. Bentley, and J. M. Harris. Chemistry for peptide and protein PEGylation. *Advanced Drug Delivery Reviews*, 54(4):459–476, June 2002.

[79] Einar K. Rofstad, Kanthi Galappathi, and Berit S. Mathiesen. Tumor interstitial fluid pressure—a link between tumor hypoxia, microvascular density, and lymph node metastasis. *Neoplasia*, 16(7):586–594, July 2014.

[80] Eric Rowinsky. The taxanes. 2003.

[81] Bernard Ryan and Gerard McCann. Novel sub-ceiling temperature rapid depolymerization-repolymerization reactions of cyanoacrylate polymers. *Macromolecular Rapid Communications*, 17(4):217–227, 1996.

[82] Gaurav Sahay, Daria Y. Alakhova, and Alexander V. Kabanov. Endocytosis of nanomedicines. *Journal of Controlled Release*, 145(3):182–195, August 2010.

[83] Howard M. Shapiro. *Practical Flow Cytometry.* John Wiley & Sons, February 2005.

[84] Sofie Snipstad. Mechanisms for delivery of hydrophobic drugs from polymeric nanoparticles to cancer cells. *Master thesis dep.physics NTNU*, 2013.

[85] Harald Stenmark. Rab GTPases as coordinators of vesicle traffic. *Nature Reviews. Molecular Cell Biology*, 10(8):513–525, August 2009.

[86] Gert Storm, Sheila O. Belliot, Toos Daemen, and Danilo D. Lasic. Surface modification of nanoparticles to oppose uptake by the mononuclear phagocyte system. *Advanced Drug Delivery Reviews*, 17(1):31–48, October 1995.

[87] Erica Strable, Jeff W. M. Bulte, Bruce Moskowitz, Kannan Vivekanandan, Mark Allen, and Trevor Douglas. Synthesis and characterization of soluble iron oxide-dendrimer composites. *Chemistry of Materials*, 13(6):2201–2209, 2001.

[88] Klaus Strebhardt and Axel Ullrich. Paul ehrlich's magic bullet concept: 100 years of progress. *Nature Reviews Cancer*, 8(6):473–480, June 2008.

[89] Einar Sulheim. *Mechanisms of Cellular Uptake and Intracellular Degradation of Polymeric Nanoparticles.* Institutt for fysikk, 2014.

[90] J. A. Swanson and C. Watts. Macropinocytosis. *Trends in Cell Biology*, 5(11):424–428, November 1995.

[91] P. Taylor. Ostwald ripening in emulsions. *Advances in Colloid and Interface Science*, 75(2):107–163, April 1998.

[92] Jiaher Tian and Valentino J. Stella. Degradation of paclitaxel and related compounds in aqueous solutions III: Degradation under acidic pH conditions and overall kinetics. *Journal of Pharmaceutical Sciences*, 99(3):1288–1298, March 2010.

[93] Katherine Tkaczuk and Jean Yared. Update on taxane development: new analogs and new formulations. *Drug Design, Development and Therapy*, page 371, December 2012.

[94] A. Tuncel, H. Çiçek, M. Hayran, and E. Pişkin. Monosize poly(ethylcyanoacrylate) microspheres: Preparation and degradation properties. *Journal of Biomedical Materials Research*, 29(6):721–728, June 1995.

[95] Kathryn E. Uhrich, Scott M. Cannizzaro, Robert S. Langer, and Kevin M. Shakesheff. Polymeric systems for controlled drug release. *Chemical Reviews*, 99(11):3181–3198, November 1999.

[96] Amir K. Varkouhi, Marije Scholte, Gert Storm, and Hidde J. Haisma. Endosomal escape pathways for delivery of biologicals. *Journal of Controlled Release*, 151(3):220–228, May 2011.

[97] Serguei V Vinogradov, Tatiana K Bronich, and Alexander V Kabanov. Nanosized cationic hydrogels for drug delivery: preparation, properties and interactions with cells. *Advanced Drug Delivery Reviews*, 54(1):135–147, January 2002.

[98] C. W. Wade and F. Leonard. Degradation of poly(methyl 2-cyanoacrylates). *Journal of Biomedical Materials Research*, 6(3):215–220, May 1972.

[99] Harris Wang, The Vo, Ali Hajar, Sarah Li, Xinmei Chen, Amadeo M. Parissenti, David N. Brindley, and Zhixiang Wang. Multiple mechanisms underlying acquired resistance to taxanes in selected docetaxel-resistant MCF-7 breast cancer cells. *BMC Cancer*, 14(1):37, January 2014.

[100] L. G. Wang, X. M. Liu, W. Kreis, and D. R. Budman. The effect of antimicrotubule agents on signal transduction pathways of apoptosis: a review. *Cancer Chemotherapy and Pharmacology*, 44(5):355–361, 1999.

[101] Sara Westrom. Cellular interaction with polymeric nanoparticles: The effect of PEGylation and monomer composition, 2013.

[102] WHO. Factsheet nr 297.

[103] Gregory J. Wiepz, Francis Edwin, Tarun Patel, and Paul J. Bertics. Methods for determining the proliferation of cells in response to EGFR ligands. *Methods in Molecular Biology (Clifton, N.J.)*, 327:179–187, 2006.

[104] Yan Xiao, Xiugong Gao, Oleh Taratula, Stephen Treado, Aaron Urbas, R. David Holbrook, Richard E. Cavicchi, C. Thomas Avedisian, Somenath Mitra, Ronak Savla, Paul D. Wagner, Sudhir Srivastava, and Huixin He. Anti-HER2 IgY antibody-functionalized single-walled carbon nanotubes for detection and selective destruction of breast cancer cells. *BMC Cancer*, 9(1):351, October 2009.

Appendices

Appendix A

Uptake

While doing DNA measurements in the flow cytometer, the uptake of NR668 was simultaneously investigated with excitation at $\lambda = 561$ nm and emission at $\lambda = 620 \pm 30$ nm. The concentration of nanoparticles was too low to detect uptake, but the cells starts to produce autofluorescence at this wavelength when they are unhealthy, as seen in figure A.1

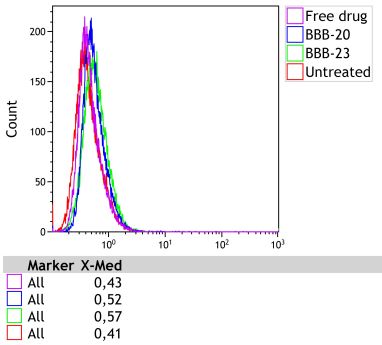

(a) 12 hours incubation.

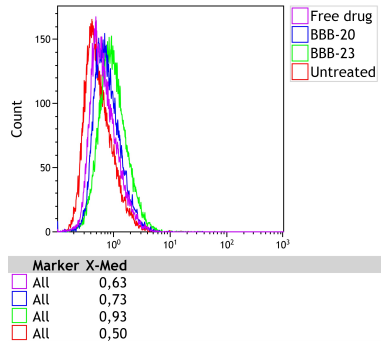

(b) 36 hours incubation.

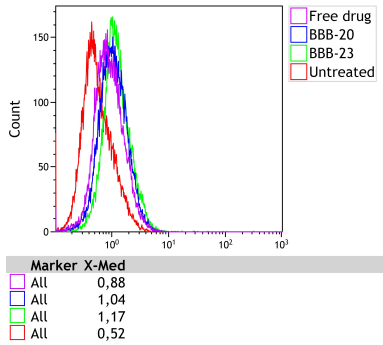

(c) 70 hours incubation.

Figure A.1: Histograms of the fluorescence detected at $\lambda = 620 \pm 30$ nm when exciting with a laser at $\lambda = 561$ nm, which is a standard way of measuring uptake of NPs. BBB-20 is loaded with both NR668 and cabazitaxel, while BBB-23 is loaded with NR668. The concentration of BBB-20 and BBB-23 is 2 μg/mL, while the concentration of free drug matches the concentration of drug in 2 μg/mL of BBB-20.

Appendix B

Initial alamarBlue results

Before optimizing the AB assay and finding the appropriate doses, there was some experiments conducted with various free and encapsulated drug concentrations and different controls. Figure B.1 shows the result from one of these. The empty PBCA NPs at 20 μg/mL (treatment B) are toxic to the cells, which was a bit unexpected. Since there is no evident increase in cytoxicity of drug concentrations from 25 ng/mL to 1000 ng/mL, the cells may be saturated with the drug.

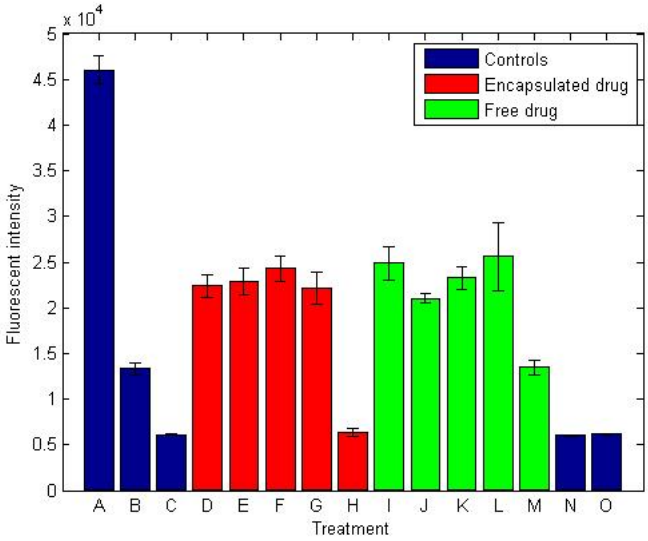

Figure B.1: Initial results from cytotoxic studies of cabazitaxel with the AB assay and 72 hours incubation. Treatments were A) Untreated, B) 20 μg/mL BBB-23, C) 100 μg/mL BBB-23, D) 0.5 μg/mL BBB-20, E) 1 μg/mL BBB-20, F) 4 μg/mL BBB-20, G) 20 μg/mL BBB-20, H) 100 μg/mL BBB-20, I) 0,025 μg/mL free drug, J) 0,05 μg/mL free drug, K) 0,2 μg/mL free drug, L) 1 μg/mL free drug, M) 5 μg/mL free drug, N) Triton and O) AB+Medium. The amount of encapsulated drug correlate with the amount of free drug, meaning that D) and I), E) and J), etc. have the same drug concentrations.